Supplementary Material

Fordyce, R. E. and Marx, F. G. 2012. The pygmy right whale *Caperea marginata* - the last of the cetotheres.

Contents

1. Data collection and cladistic methodology

Almost all characters were scored directly from specimens, rather than from the literature. To clarify character states and ensure the repeatability of our work, virtually every scoring in the data matrix was illustrated with photographs on MorphoBank [29,30], project 578, with the exception of *Morenocetus parvus* , which is currently under re-description by M. Buono. The molecular partition of our data set included 13,535 mitochondrial (mt) and 28,005 nuclear (nu) nucleotide characters, as well as 694 gap characters and 101 transposon insertion events, pruned to match the taxa in our analysis (note that these numbers represent the dimensions of the original data matrix of [10]; however, several of these characters were missing for the taxa in our data set). The complete data matrix is available on MorphoBank.

We used the “traditional search” option of TNT (v.1.1) [31,32] to perform a heuristic parsimony analysis of the morphological data based on 10,000 random stepwise-addition replicates and tree bisection reconnection (TBR) branch swapping, saving 10 trees per replicate. The total evidence analysis combining the morphological and molecular data was carried out using Markov Chain Monte Carlo (MCMC) Bayesian analyses implemented in MrBayes v.3.2.1 [33,34], with four

simultaneous chains (one cold, three heated) and three concurrent runs of 12.0 x 10^6 generations (sampled every 500 generations). The mt, nu, gap, transposon and morphological data were treated as separate partitions. We used jModelTest v.0.1.1 [35,36] to choose optimal nucleotide substitution models for the mt and nu partitions (both GTR + G). Gaps and transposons were analysed under the binary model of character evolution implemented in MrBayes, while the morphological data used the maximum likelihood model for morphological data [37] assuming equal rates of change among characters. A second analysis allowing for variable rates based on a gamma distribution was also run and compared to the equal-rates analysis using Bayes factors (BF), calculated as twice the difference between the logarithms of the harmonic means of the model likelihoods [38,39]. The results of both analyses were virtually identical (the results of the variable-rates analysis were slightly less resolved), and there was very strong evidence (*sensu* [40]) favoring the variable-rates (gamma) model over the equal-rates one (BF=14.92). Therefore, only the results of the variable-rates analysis are reported here. Convergence was assessed using the standard deviation of split frequencies (with convergence being assumed once the latter fell and stayed below 0.01), as well as (cumulative) split frequencies and symmetric tree-difference scores plotted in AWTY [41]. For all analyses, the first 25% of generations were discarded as burn-in.

2. Stratigraphic ranges of *Cetotherium rathkii*, *Metopocetus durinasus, Morenocetus parvus, Nannocetus eremus* and *Piscobalaena nana*

Cetotherium rathkii was described based on a single specimen from the Sarmatian of Ukraine [38]. In the region of the Central Paratethys, the Sarmatian Stage as a whole has been assigned the Middle Miocene [42]. By contrast, in the eastern Paratethys the upper part of the Sarmatian correlates with the early Tortonian [42–44]. Although the precise stratigraphic context is currently unknown, the type specimen of *C. rathkii* likely originated from strata assignable to the upper part of the Sarmatian, and hence the early Tortonian [Gol'din 2012, pers. comm.].

Metopocetus durinasus is known from a single specimen, collected from "a Miocene marl from near the mouth of the Potamac river" [45:143]. Subsequent

authors interpreted the original description of the type locality to refer to either the Calvert Formation [46] or the St. Mary's Formation [47], thus implying either a Langhian (13.8–16 Ma) or early Tortonian (9.4–11.6 Ma) age, respectively [48−50].

Morenocetus parvus is known from two specimens from lower part of the Gaiman Formation of Patagonia, Argentina [20]. In the area of the type locality of *M. parvus*, the lower part of Gaiman Formation overlies the continental Sarmiento Formation, which contains a mammal fauna correlating with the Colhuehuapian South American Land Mammal Age [51,52]. The latter was dated to 19.8-20.9 Ma, based on 40Ar/39Ar dating [53], thus providing a maximum age of ca. 20 Ma (earliest Burdigalian) for the lower part of the Gaiman Formation in this area. Since virtually all vertebrate material recovered so far originated from the lowermost levels of the Gaiman Formation, close to its contact with the Sarmiento Formation (Cozzuol 2010, pers. comm.), the age of *Morenocetus* is here assumed to be early Burdigalian.

Nannocetus eremus is known from two crania from the Late Miocene of California [19,54]. Though originally reported as having been recovered from the Early Pliocene Pico Formation [54], the holotype skull likely derives from the basal part of the Towsley Formation [19], which has been dated to the Messinian [55]. A second, referred specimen was later found in the upper part of the Santa Margarita Formation [19; Boessenecker 2012, pers. comm.], dated to about 9 Ma based on the faunal content of nearby localities [56:26–27]. This extends the range of *Nannocetus* to the late Tortonian [57].

Piscobalaena nana is known from several specimens from the Late Miocene localities of Sud-Sacaco and Aguada de Lomas, both contained within the Pisco Formation of Peru [7]. Originally thought to date to the Early Pliocene [7], recent work assigned Sud-Sacaco to the Late Miocene (6–7 Ma, Messinian) based on $^{87}Sr/^{86}Sr$ dating [58]. By contrast, the locality of Agua de Lomas is somewhat older (7–8 Ma) based on K-Ar dating [7,59], thus extending the range of *P. nana* to the late Tortonian.

3. Comparisons with recent analyses discussing *Caperea* relationships

The evolutionary relationships of *Caperea* were extensively discussed by three recent analyses focusing on balaenid systematics, the ear bone morphology of extant mysticetes, and baleen whale cladistics, respectively [13–15]. Two of these studies supported the long-held morphological view of a clade comprising *Caperea* and balaenids [13,14], while the third discussed and largely rejected most previously proposed synapomorphies of a *Caperea*-balaenid clade, and instead suggested a relationship of *Caperea* with eschrichtiids and balaenopterids, but not cetotheres [15].

Characters hitherto proposed to support a close relationship of *Caperea* and balaenids include: a rectangular anterolateral margin of the maxilla ([13]:char. 10); palatal maxillary sulci opening into a long alveolar groove ([13]:char. 16); a poorly developed hamular process of the pterygoid ([13]:char. 31); exclusion of the parietals from the vertex by the supraoccipital ([13]:char. 36); a short ([13]:char. 44) and laterally oriented ([13]:char. 45) zygomatic process of the squamosal; a far anteriorly projected supraoccipital shield ([13]:char. 49); a compound posterior process of the tympanoperiotic oriented at a right angle to the long axis of the pars cochlearis ([14]:char. 25); a rhomboid ([13]:char. 57; [14]:char. 1) and dorsoventrally compressed ([13]:char. 58) tympanic bulla; a weakly developed conical process of the tympanic bulla ([13]:char. 62; [14]: char. 14); a short anterior lobe of the tympanic bulla ([14]:char. 14); a dorsally directed mandibular condyle ([13]:char. 80); fusion of the cervical vertebrae ([13]:char. 93); and a skull length greater than 25% of the total body length ([13]:char. 114).

Out of the above, a far anteriorly projected supraoccipital shield (char. 50 of the present study) and fusion of the cervical vertebrae (char. 152) are consistent with the findings of this study, and remain as potential synapomorphies of a *Caperea*-balaenid clade. A short zygomatic process of the squamosal and a skull length exceeding 25% of the total body length also might represent potential synapomorphies. However, the zygomatic process of balaenids, though short, is massive, cylindrical, and relatively well-developed, thus differing from the extremely short and deep zygomatic process of *Caperea* (figures S3A, S4A,C). Furthermore, a

skull length exceeding 25% of the total body length is not exclusive to *Caperea* and balaenids and also occurs in, for example, *Megaptera novaeangliae* [60].

By contrast, a poorly developed hamular process of the pterygoid, a laterally oriented zygomatic process, and a compound posterior process oriented at a right angle to the long axis of the pars cochlearis, as well as most likely a dorsoventrally compressed bulla and a dorsally oriented articular surface of the mandibular condyle, are not observed in *Caperea* (see discussion of chars. 54, 74, 109, 132 and 148 below). Conversely, a short anterior lobe is absent in *Eubalaena*, and instead is present in a range of other non-balaenid species (char. 113). A rhomboid bulla (char. 112) and a low conical process (char. 120) are not exclusive to *Caperea* and balaenids, and instead also occur in herpetocetines. Finally, the exclusion of the parietals from the vertex is likely a consequence of the forwards projection of the supraoccipital (char. 50), while a rectangular anterolateral margin of the maxilla and the presence of a palatal “alveolar” groove are likely a consequence of rostral compression (char. 3) and the resulting realignment and confluence of palatal sulci associated with baleen nutrient foramina, as shown by the incomplete confluence of the sulci in several specimens of *Caperea* (e.g. OM VT227) and *Eubalaena* (e.g. FMNH 15559; MSNTUP M263).

Characters proposed to support a close relationship of *Caperea* with eschrichtiids and balaenopterids include a narrow anterior portion of the premaxilla ([15]:char. 7); a posteriorly directed supraorbital process ([15]:char. 28); abrupt depression of the supraorbital processes ([15]:char. 31); a supraorbital process whose medial portion exceeds its lateral portion in anteroposterior length ([15]:char. 33); the presence of a squamosal cleft ([15]:char. 75); and cranial elongation of the pars cochlearis ([15]:char. 84).

Out of the former, the presence of a squamosal cleft (char. 68 below) remains as potential synapomorphy of a *Caperea*-balaenopteroid clade. By contrast, a narrow anterior portion of the premaxilla (char. 4) and a posteriorly pointing supraorbital process (char. 23) are variably developed among mysticetes, and also occur in balaenids. Furthermore, although the medial portion of the supraorbital process of *Caperea* exceeds its distal portion in anteroposterior length, the anterior and posterior borders of the supraorbital are roughly parallel. In this, *Caperea*

resembles balaenids, some balaenopterids, and several extinct Miocene taxa of uncertain familial affinity, and clearly contrasts with the much more medially elongate, trapezoidal supraorbital processes of *Balaenoptera musculus*, *Megaptera novaeangliae* and several extinct balaenopterids. Finally, we agree with previous studies [13,14] that the abrupt depression of the supraorbital process (char. 25) and the cranial elongation of the pars cochlearis (char. 84) in *Caperea* are based on debatable interpretations of morphology. Although the supraorbital process of *Caperea* is depressed below the vertex, the frontal lacks a clear division in a vertically oriented medial and a horizontally oriented lateral portion, as observed in *Eschrichtius* and balaenopterids. Instead, the frontal is relatively low in lateral view, with the lateral wall of the skull dorsal to the supraorbital process formed by the parietal only. Similarly, while the pars cochlearis of adult *Caperea* does show a form of cranial elongation, the latter is usually limited to the anteriormost part of the pars cochlearis, thus differing from the more broadly developed elongation observed in *Eschrichtius* and balaenopterids (figure S5).

In summary, most of the morphological evidence presented in favor of a close relationship of *Caperea* with balaenids or balaenopterids thus either seems questionable in light of our observations, or instead also supports a clade comprising *Caperea* and cetotheres.

4. Discussion of specific characters

Char. 13 Lateral borders of ascending process of maxilla: in adult specimens of both *Caperea* and balaenids, the forwards projection of the supraoccipital has reduced the ascending processes of the maxillae to short, barely noticeable projections, thus resulting in a superficial resemblance of these two taxa. However, juvenile *Caperea* preserve a clearly distinguishable, parallel-sided ascending process (figure S1). In this, *Caperea* differs from balaenids, in which the ascending process is short and broadly triangular even in juveniles [61:pl. 1-2, figures 7,8]. These observations imply that the reduction of the ascending process of *Caperea* and balaenids fails the test of primary homology [62–64], and should therefore be coded separately. Given the resemblance of the ascending process of juvenile *Caperea* to that of balaenopterids and cetotheres, we thus decided to code *Caperea* the same as the latter two taxa.

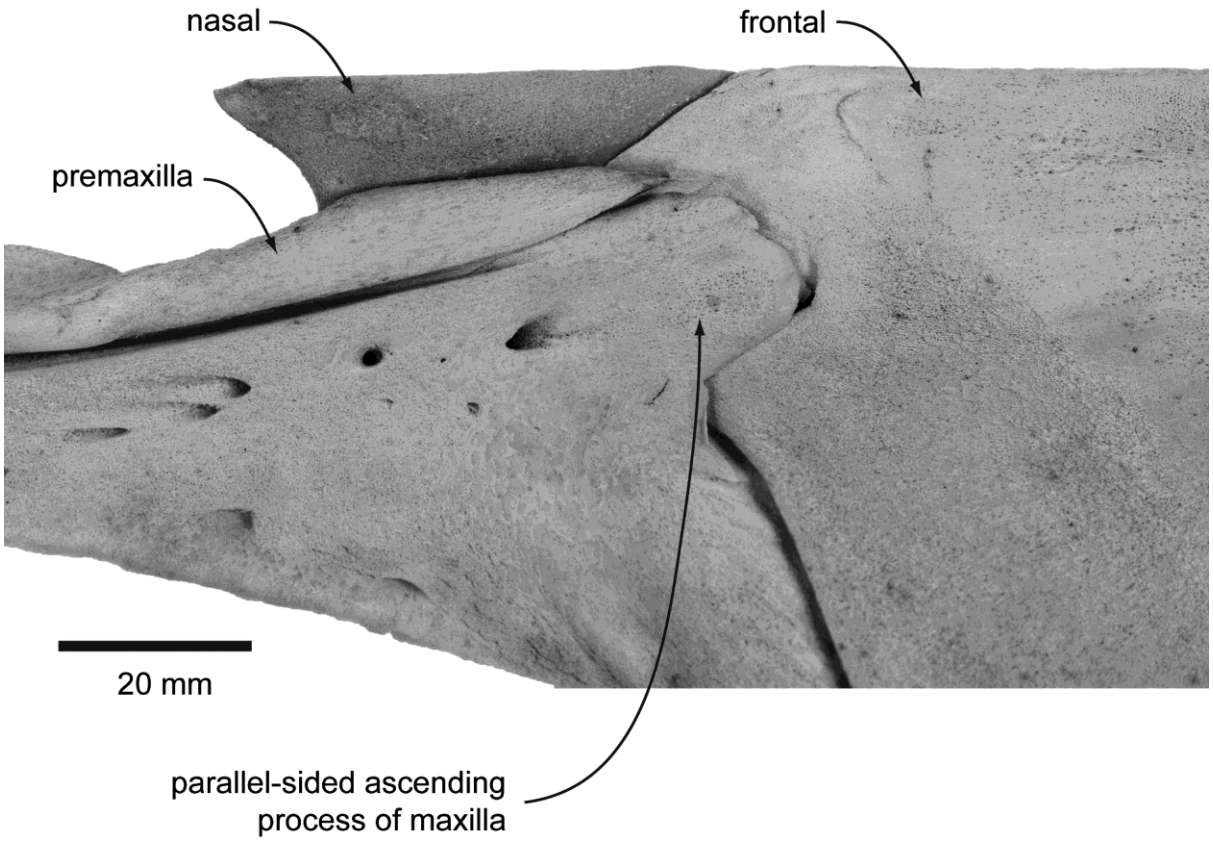

Figure S1 Dorsal view of a neonate specimen of *Caperea marginata* (NMNZ MM002898), showing the parallel-sided ascending process of the left maxilla.

We tested the effects of this decision on our results by performing a separate analysis of our morphological data with *Caperea* instead coded as having a triangular ascending process (as seen in *Caperea* adults, balaenids and several fossil taxa). The results of this analysis were identical to those presented in the main text, with the exception of slightly lower symmetric resampling values for Cetotheriidae and the successive sub-clades within the latter leading up to *Caperea*.

Char. 38 Anterior margins of nasals: in *Caperea*, *Piscobalaena* and a referred specimen of *Herpetocetus* (UCMP 219111; Boessenecker 2012, pers. comm.), as well as *Megaptera novaeangliae*, the anterior margins of the nasal converge towards the sagittal plane, thus forming a medial tip clearly separated from the premaxillae in dorsal view (figures 1A, S2A, B). By contrast, the anterior margins of the nasals are evenly grooved in most balaenids, resulting in a distinct W-shape (figure S2C), while being straight or slightly rounded in most other mysticetes.

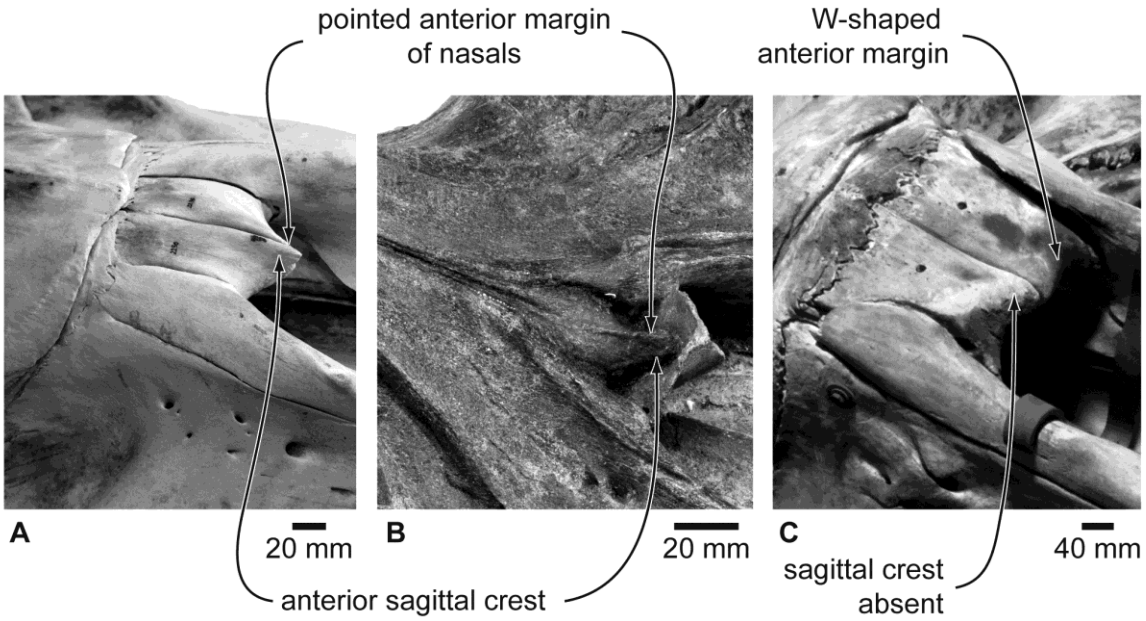

Figure S2 Dorsolateral view of the nasals of (A) *Caperea marginata* (NMNZ MM0022235), (B) *Piscobalaena nana* (MNHN SAS1617) and (C) *Eubalaena australis* (USNM 267612).

Char. 39 Dorsal surface of nasals: the anterodorsal surface of the nasals bears a sagittal crest in *Caperea*, *Piscobalaena*, a referred specimen of *Herpetocetus* (UCMP 219111; Boessenecker 2012, pers. comm.), *Eschrichtius robustus*, and *Megaptera novaeangliae* (figure S2A,B). This contrasts with the condition in most other mysticetes, including non-herpetocetine cetotheres (e.g. *Metopocetus durinasus*), in which the dorsal surface of the nasals is flattened (figure S2C).

Char. 42 Zygomatic process of squamosal and exoccipital in dorsal view: in *Herpetocetus*, *Nannocetus*, *Caperea*, *Eschrichtius* and balaenids, the lateral edge of the exoccipital, the tip of the compound posterior process of the tympanoperiotic and the lateral edge of the zygomatic process of the squamosal lie roughly in the same plane, thus forming a continuous, unbroken lateral skull border (figure 1A,C) [19]. By contrast, the zygomatic process of other mysticetes, including non-herpetocetine cetotheres, is laterally offset from the lateral edge of the exoccipital and the compound posterior process, resulting in the formation of a distinct angle and re-entrant in the lateral skull border.

Char. 50 Anteriormost point of supraoccipital in dorsal view: previous analyses have tended to code this character independently from characters dealing with the

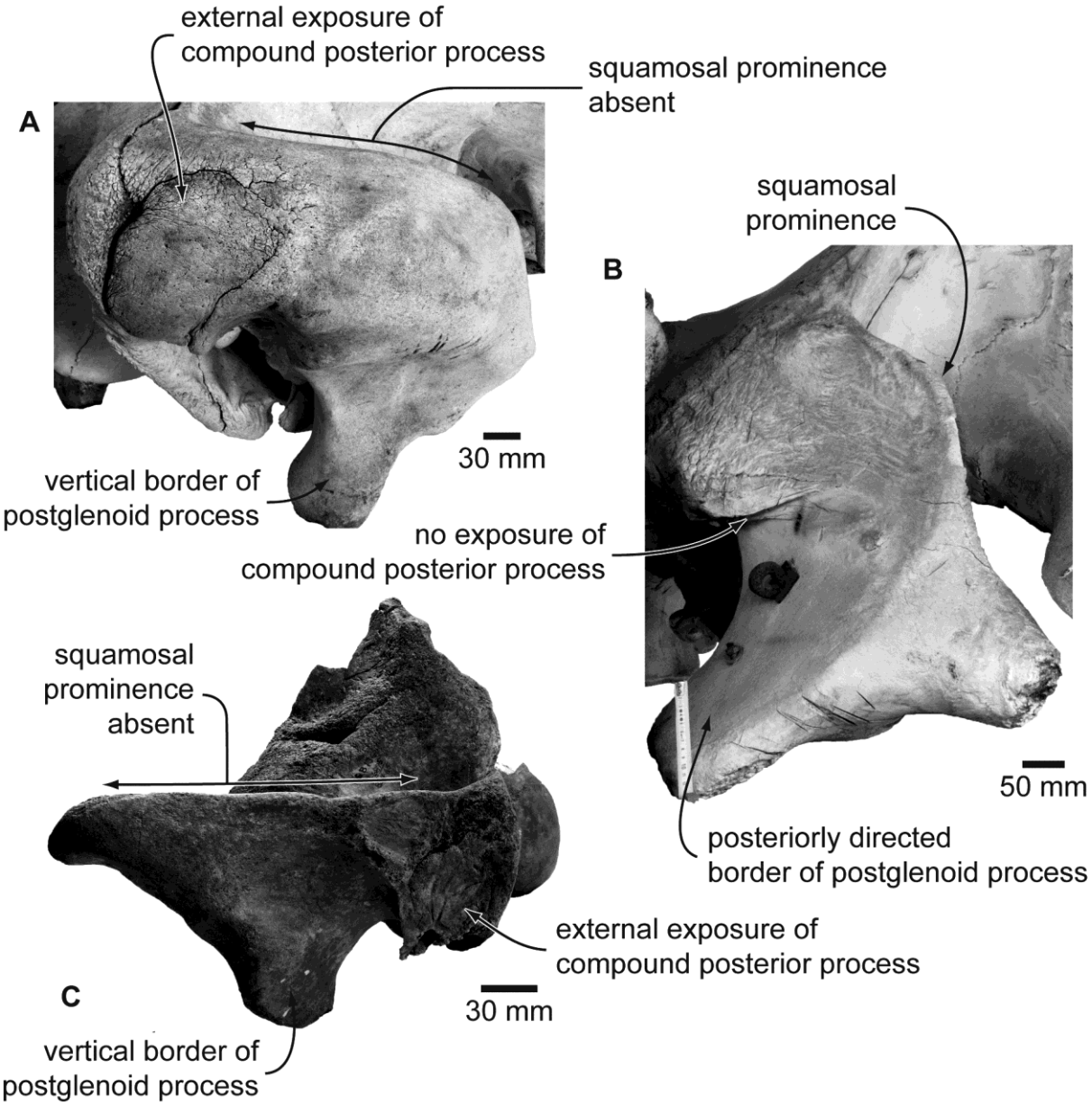

Figure S3 Posterolateral view of the right squamosal of (A) *Caperea marginata* (OM VT227), and (B) *Eubalaena glacialis* (MSNTUP M264), and the left squamosal of (C) *Herpetocetus bramblei* (UCMP 82465).

morphology of the posterior portion of the rostral bones, such as the position of the posterior border of the maxillae (char. 33) and nasals (char. 41), or the separation of the ascending processes of the maxillae (char. 34) [9,15,26]. This is problematic, as the forwards projection of the supraoccipital shield in taxa such as balaenids, "*Megaptera*" *miocaena* and *Caperea* likely predetermines the position of the posterior borders of the rostral bones: if the supraoccipital extends to the base of the rostrum, the rostral bones cannot physically extend towards the back of the skull as

seen in, for example, balaenopterids or cetotheres [7,8,15]. Similarly, a forwards-projected supraoccipital leaves little room for contacting ascending processes of the maxillae, as also seen in cetotheres. Apart from obscuring other possible relationships, this link between an anteriorly projected supraoccipital and the absence of any posterior telescoping of the rostral bones may have biased previous analyses towards a clade including both balaenids and *Caperea* by overweighting the position of the supraoccipital through a suite of linked characters. We therefore decided to code some characters describing aspects of the rostral elements as non-applicable in taxa with an anteriorly positioned supraoccipital (see notes on MorphoBank, project 578).

Other characters also likely affected by the degree of telescoping of the supraoccipital are (1) the exposure of parietals on the skull vertex and (2) the degree to which the lateral borders of the supraoccipital overhang the lateral walls of the skull. As for (1), the exposure of the parietals on the vertex must necessarily decrease in taxa with a far anteriorly positioned supraoccipital, or far posteriorly extending rostral elements, thus linking this character to the degree of telescoping of these bones. As for (2), the lateral borders of the supraoccipital tend to overhang the lateral walls of the skull in taxa with relatively far anteriorly projected supraoccipital shields, such as balaenids, balaenopterids, and *Caperea*. By contrast, taxa with a posteriorly positioned supraoccipital, such as toothed mysticetes and cetotheres, tend to show a relatively small, if any, degree of overhang of the supraoccipital. This observation makes sense given the triangular or rounded outline of the supraoccipital shield in mysticetes, which would likely result in an increasing degree of overhang as the broader posterior portions are stretched anteriorly during telescoping. Owing to these potential links, we decided not to code the exposure of the parietal and the degree of occipital overhang in our analysis.

Char. 54 Orientation of zygomatic process of squamosal: the zygomatic process of *Caperea* differs from that of all other mysticetes in being both extremely short anteroposteriorly and extremely high dorsoventrally (figures S3A, S4A). Although the great degree of anteroposterior reduction makes an accurate assessment of the orientation of the zygomatic process itself difficult, the anteroposterior alignment of the lateral surface of the exoccipital, the lateral border of the squamosal fossa, and the orbit (figure 1A) strongly suggest an anterior orientation for the remnant of the

zygomatic process, resembling other cetotheres, *Eschrichtius*, most balaenopterids, and most extinct Miocene taxa of uncertain familial affinity, such as *Diorocetus*. By contrast, the zygomatic process is oriented distinctly anterolaterally in balaenids (figure S4C) and *Megaptera novaeangliae*, and somewhat anteromedially in toothed mysticetes.

Char. 60 Squamosal prominence: in most mysticetes, the squamosal prominence, sometimes also referred to as the lateral squamosal crest [12], is present as projection on the lateral or posterolateral border of the squamosal fossa. The prominence is particularly well-developed in balaenids, in which it forms a large, semicircular process. By contrast, the prominence is reduced or absent in herpetocetines, *Piscobalaena*, *Caperea*, and some balaenopterids, resulting in a straight or slightly undulating dorsolateral border of the squamosal fossa (figure S3).

Char. 63 Postglenoid process in lateral view: the lateral outline of the postglenoid process of the squamosal varies widely among mysticetes. In herpetocetines [19] and *Caperea*, the postglenoid process is triangular in lateral view, with the posterior border being vertical or descending anteroventrally (figure S3A,C). The postglenoid process is also triangular in *Eschrichtius* and some non-herpetocetine cetotheres, as well as some extinct Miocene taxa, such as *Pelocetus calvertensis*, although in these taxa the tip of the process points posteriorly. By contrast, the postglenoid process is curved anteriorly in early toothed mysticetes, while forming a plate with parallel anterior and posterior borders in extant balaenopterids (with the tip of the process pointing ventrally) and balaenids (with the tip pointing posteriorly, figure S3B).

Char. 70 Sagittal crest on supraoccipital shield: in *Caperea*, *Piscobalaena* and a referred specimen of *Herpetocetus* (UCMP 219111; Boessenecker 2012, pers. comm.), the supraoccipital shield is marked by a prominent sagittal crest running all or most of the way from the apex of the supraoccipital to the occipital condyles. The same crest is variably developed in other mysticetes, ranging from being absent in balaenids, some balaenopterids, and some Miocene taxa (e.g. *Pelocetus calvertensis*), to a well-developed crest restricted to the anterior half or the area immediately posterior to the apex of the supraoccipital shield in toothed mysticetes, *Eomysticetus*, some balaenopterids, and some Miocene species (e.g. *Diorocetus hiatus*).

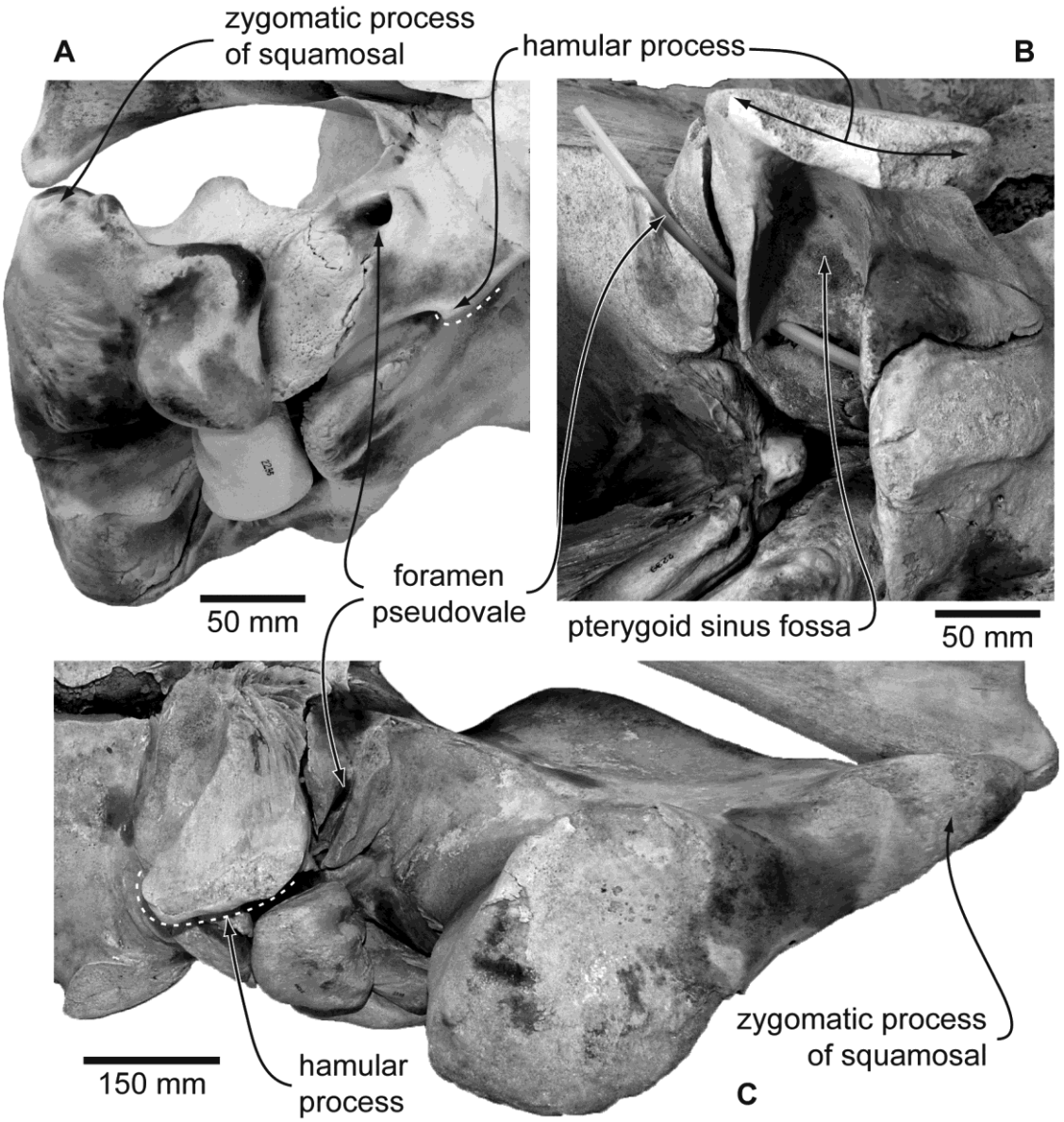

Figure S4 Hamular process of (A) *Caperea marginata* (NMNZ MM002235) in ventral view, and (B-C) *Eubalaena australis* (NMNZ MM002239) in posterior (B, right side) and ventral (C, left side) views. Also note the different morphology of the zygomatic process of the squamosal in these two taxa.

Char. 74 Shape of pterygoid hamuli: the hamular processes of *Caperea* are unique among mysticetes in having been reduced to small, obliquely oriented, peg-like projections. This contrasts with the well-developed, finger-like hamuli of balaenopterids, the slender but long hamuli of most extinct mysticetes, and the broad, dorsoventrally flattened, plate-like hamular processes flooring the pterygoid sinus and underlying the posterior portions of the palatines in balaenids [65].

Char. 84 Dorsal and medial elongation of pars cochlearis towards cranial cavity: *Caperea* is distinct from all other mysticetes in having a pars cochlearis showing a high degree of cranial elongation restricted to its anteriormost portion (figure S5A). In at least one individual (NMNZ MM002900), the elongated portion of the pars cochlearis is continuous with a sheet of fibrous bone flooring the anterior portion of the cranial hiatus (figure S5B). This contrasts with the situation in *Eschrichtius* and most balaenopterids, in which the pars cochlearis is elongated along most or all of its medial border (figure S5C), as well all as that in other mysticetes, in which the cranial elongation of the pars cochlearis is absent.

Char. 85 Anterior process in lateral view: in *Caperea*, *Megaptera novaeangliae*, and most specimens of *Herpetocetus*, the anterior process of the periotic is delimited by an irregular, often L-shaped anterior edge (figure 2A,B). By contrast, the process is triangular in *Eschrichtius* and most balaenopterids, while being squared or broadly rounded in most other mysticetes. Although rough patterns are discernible, this distribution and development of this feature is highly variable in both *Caperea* and *Herpetocetus*, and in need of further investigation.

Char. 92 Lateral tuberosity of anterior process: the lateral tuberosity is a lateral projection of the ventral part of the periotic situated at the base of the anterior process, lateral or anterolateral to the mallear fossa. In most mysticetes, the lateral tuberosity is developed as a relatively blunt, knob-like structure located immediately posterior to the anterior pedicle of the bulla. By contrast, the same structure is hypertrophied and forms an elongate blade in extant balaenids, while taking the shape of a shelf, located anterolateral to the anterior pedicle of the bulla and articulating with the squamosal, in herpetocetines (figures 2B, S7B).

Previous analyses reported the lateral tuberosity to be absent or featureless in *Caperea* [7,9,14]. However, the lateral tuberosity does occur in the shape of a robust anterior projection which superficially forms (and hence can easily be confused with) the lateral margin of the anterior process. In lateral view, the anterior process bears an extremely well-developed, longitudinal groove (figure S6A). The latter originates on the dorsal surface of the anterior process, dorsolateral to the poorly defined mallear fossa, and extends anteriorly almost to the tip of the process. Near its

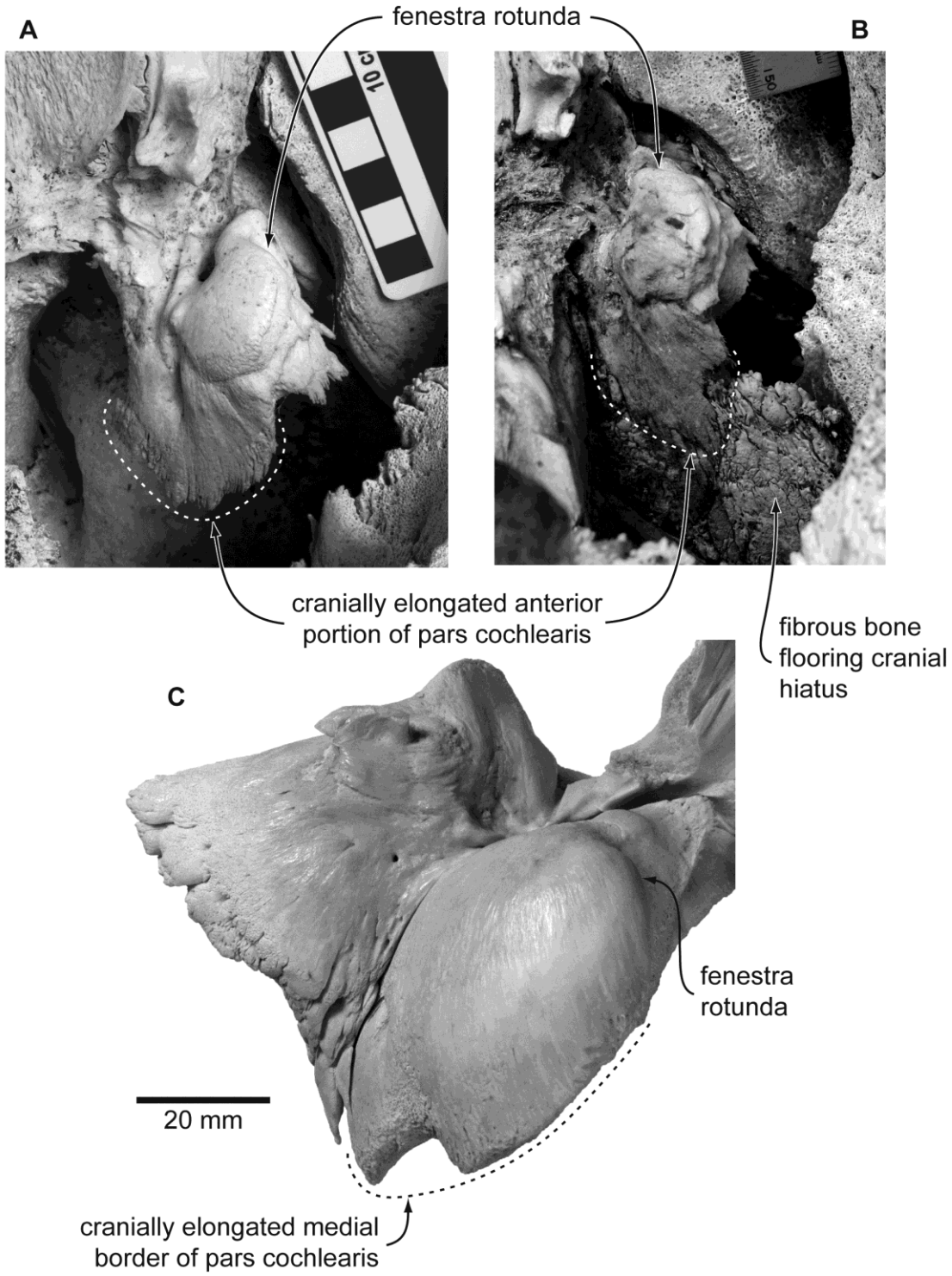

Figure S5 Cranial elongation of the pars cochlearis in lateral view in *Caperea marginata* (A, OM VT227; B, NMNZ MM002900) and (C) *Balaenoptera bonaerensis* (OM VT3057).

anterior end, the groove turns into a cleft, apparently dividing the anterior process into a medial (strictly, the anterior process of the periotic) and a lateral portion (strictly, the lateral tuberosity). In ventral view, this cleft is visible near the tip of the anterior process (figures 2A, S6B,C). Further posteriorly the cleft disappears, but in some specimens (e.g. NMV C28531) the division between the anterior process and the lateral tuberosity is still apparent in form of a groove running up to the anterior pedicle. In addition, the two structures are distinguished in ventral view by the surface texture of the bone, with anteromedially oriented striations on the surface of the anterior process portion opposing anterolaterally oriented striations on the lateral tuberosity (figure S6C). When articulated with the squamosal, the tip of the lateral tuberosity points towards the gap between the falciform and postglenoid processes of the squamosal (figures 2A, S7A).

Its origin near the anterior pedicle and the mallear fossa, as well as its articulation with the squamosal justify our interpretation of the “lateral portion” of the anterior process as homologous to the lateral tuberosity of other mysticetes. In this scenario, the lateral tuberosity of *Caperea* became re-oriented and extended far anteriorly relative to the condition in other baleen whales, forming a long, thick shelf located anterolateral to the anterior pedicle of the bulla. Although clearly distinct from the lateral tuberosity of any other taxon, this condition most closely resembles that found in herpetocetines. In the latter, the lateral tuberosity occurs as a broad, anteriorly pointing shelf situated lateral or anterolateral (as opposed to posterior) to the anterior pedicle of the bulla, and articulates with the squamosal in the same position as seen in *Caperea* (figures 2A,B, S7). The morphology of the lateral tuberosity of herpetocetines could therefore be interpreted as intermediate between that of *Caperea* and the knob-like tuberosity of most other mysticetes.

Char. 94 Anteromedial corner of pars cochlearis in ventral view: in herpetocetines, *Caperea* and *Zygorhiza kochii*, the anteromedial corner of the ventral surface of the pars cochlearis is angular in ventral view, resulting in a flattened ventral surface of the pars cochlearis (figure S8). However, whereas in *Zygorhiza* the ventral surface of the pars cochlearis is delimited by a well-developed, ventrally pointing ridge, the transition of the ventral and medial sides of the pars cochlearis is relatively more rounded in herpetocetines and *Caperea*, with only the anteromedial

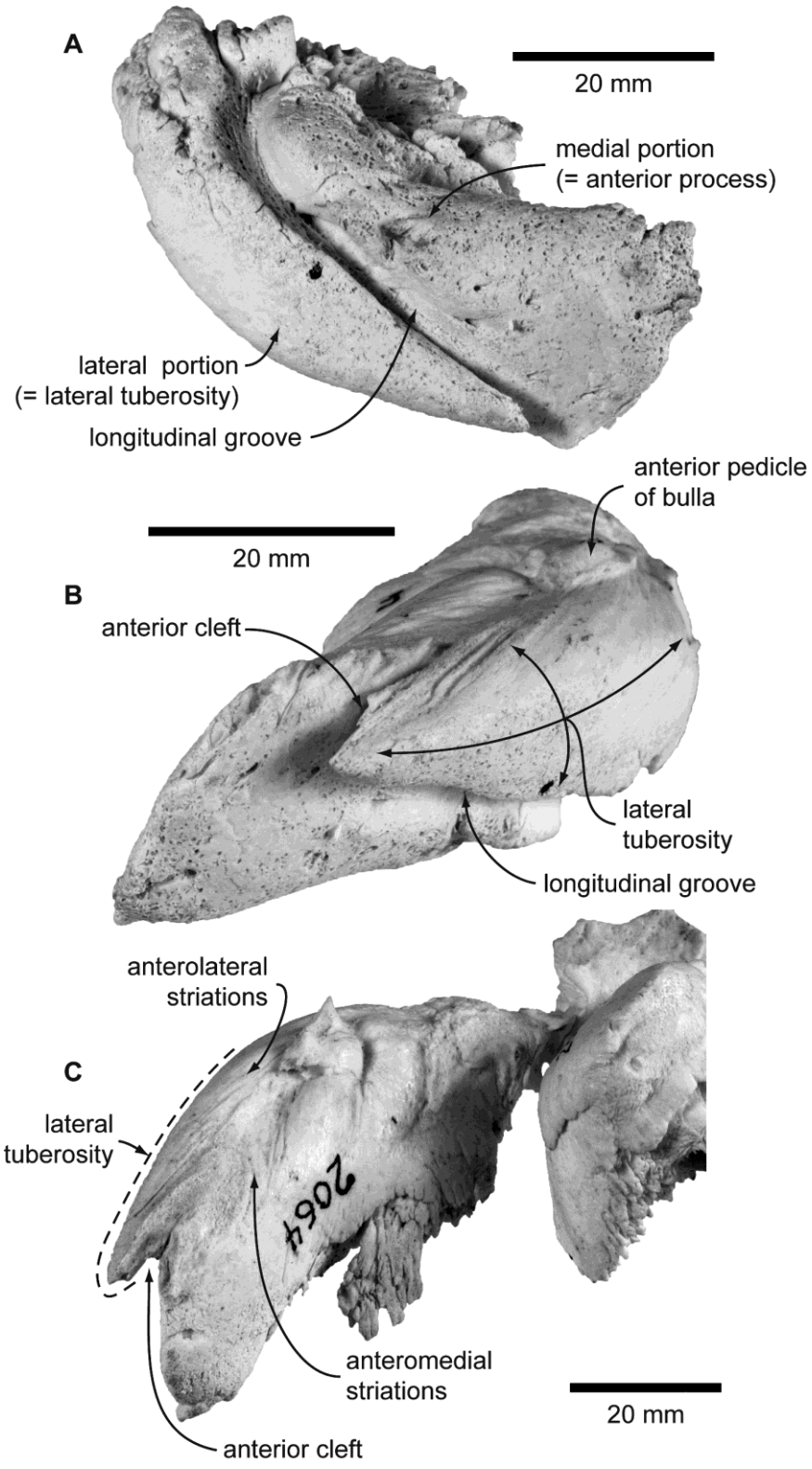

Figure S6 Right anterior process of the periotic of *Caperea marginata* (NMNZ MM002064) in (A) anterolateral and (B) ventrolateral views; (C) left anterior process in anteromedial view.

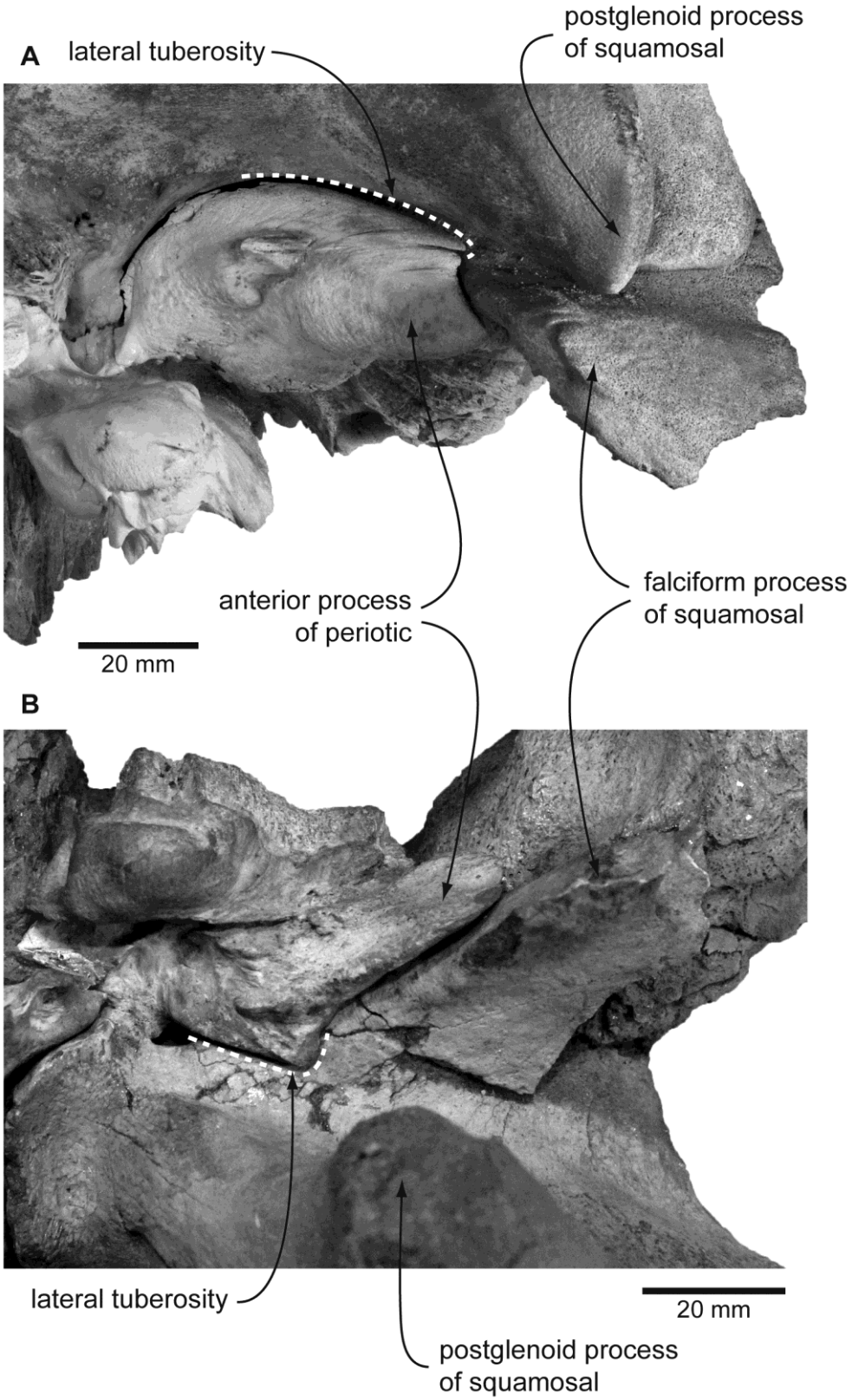

Figure S7 Ventral view of the articulated periotic and squamosal of (A) *Caperea marginata* (right periotic, NMV C28531) and (B) *Herpetocetus transatlanticus* (left periotic, USNM 182962).

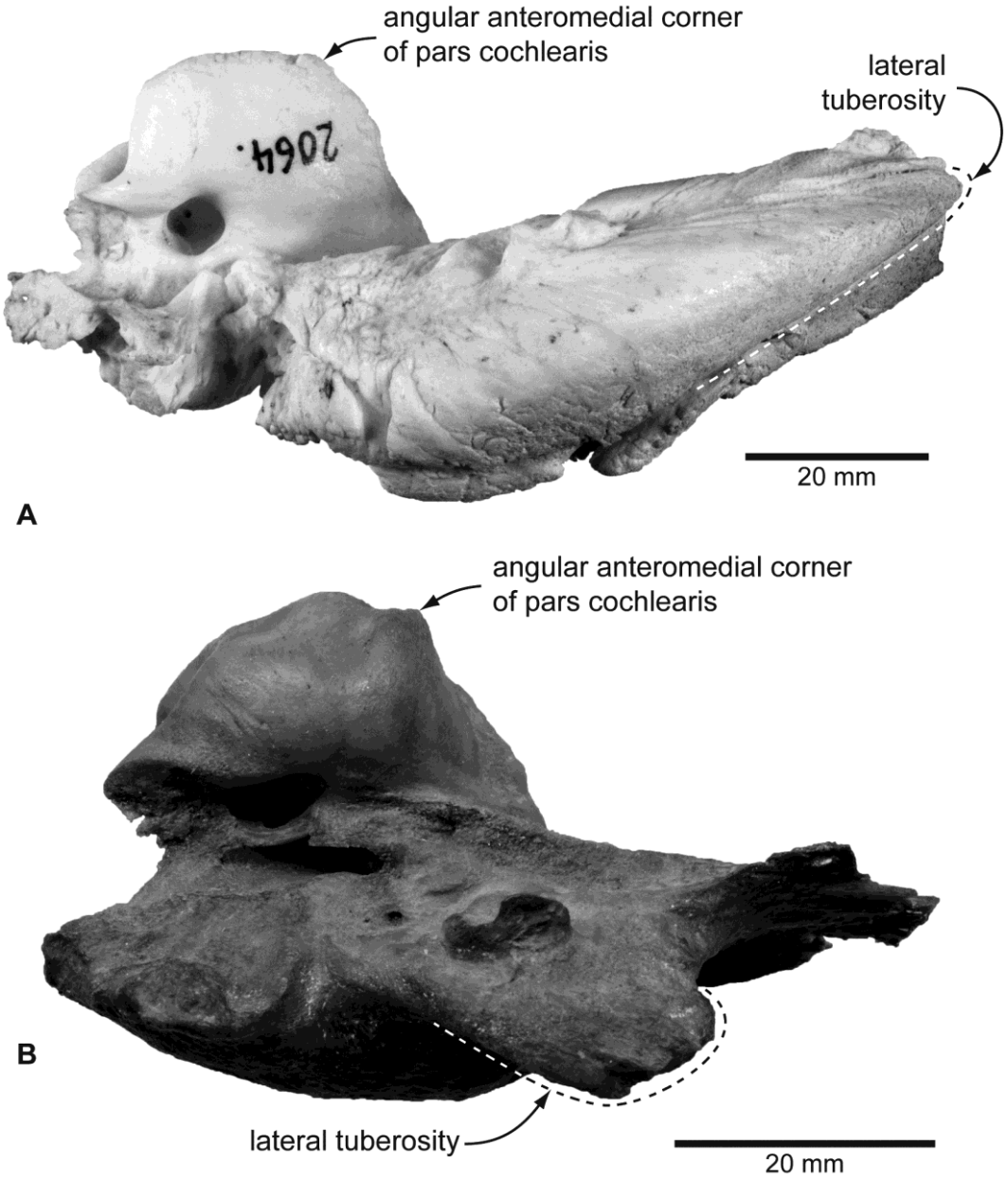

Figure S8 Ventral view of the anterior portion of the left periotic of (A) *Caperea marginata* (NMNZ MM002064) and (B) *Herpetocetus bramblei* (UCMP 82465).

corner of the pars cochlearis itself extending medially to form a small, but usually well-defined projection. By contrast, the anteromedial corner and ventral surface of the pars cochlearis of virtually all other mysticetes are rounded and indistinct.

Char. 98 Morphology of caudal tympanic process: in virtually all mysticetes, including balaenids, balaenopterids, eschrichtiids, some cetotheres and virtually all of the other Miocene fossil taxa, the caudal tympanic process forms a well-developed shelf or flange extending posteriorly from the ventral surface of the pars

cochlearis, just lateral to the fenestra rotunda. By contrast, the process is reduced or almost absent in herpetocetines and *Caperea* (figures 2A,B, S9).

The situation in Oligocene mysticetes and late Eocene archaeocetes is less clear, as the caudal tympanic process in these taxa is regularly broken, or possibly absent (e.g. *Eomysticetus whitmorei*, *Zygorhiza kochii*). However, the process is preserved and well-developed, albeit thin and fragile, in at least one undescribed eomysticetid from the late Oligocene of New Zealand (OU 12918), thus indicating that the fracture surfaces found in several other specimens of early mysticetes likely are remnants of relatively well-developed processes, too.

Char. 109 Orientation of compound posterior process in ventral view with periotic being *in situ*: in most mysticetes, including *Caperea*, the compound posterior process of the tympanoperiotic as viewed *in situ* is oriented posterolaterally with regards to the long axis of the anterior process. This contrasts with the situation in most balaenids, in which the posterior process is oriented roughly at a right angle to the anterior process (figure S10).

Chars. 110, 111 Shape of compound posterior process/ exposure of compound posterior process on lateral skull wall: in herpetocetines, *Piscobalaena*, *Metopocetus* and *Caperea*, the distal end of the compound posterior process of the periotic is distinctly wider than its more proximal portions, thus forming a “plug” (figures 1B,D–F, 2A,B, S3A,C, S10A). By contrast, the posterior process is anteroposteriorly flattened in most balaenopterids, while being roughly cylindrical or only slightly conical in most other mysticetes (figure S10B).

Although related to the shape of the compound posterior process, the exposure of the process codes a different morphology. In herpetocetines, *Piscobalaena*, *Metopocetus* and *Caperea*, the distal end of the compound posterior process bears a distinct lateral face forming part of the lateral surface of the skull. By contrast, in other reported cetotheres, such as *Joumocetus shimizui* (GMNH PV2401) [38], the posterior process is clearly exposed, but not shaped like a “plug”.

Char. 112 Anterior border of bulla in dorsal or ventral view: *Caperea*, herpetocetines, *Piscobalaena*, and balaenids are characterized by a squared anterior end of the bulla, compared to a more rounded anterior border in most other mysticetes (figure

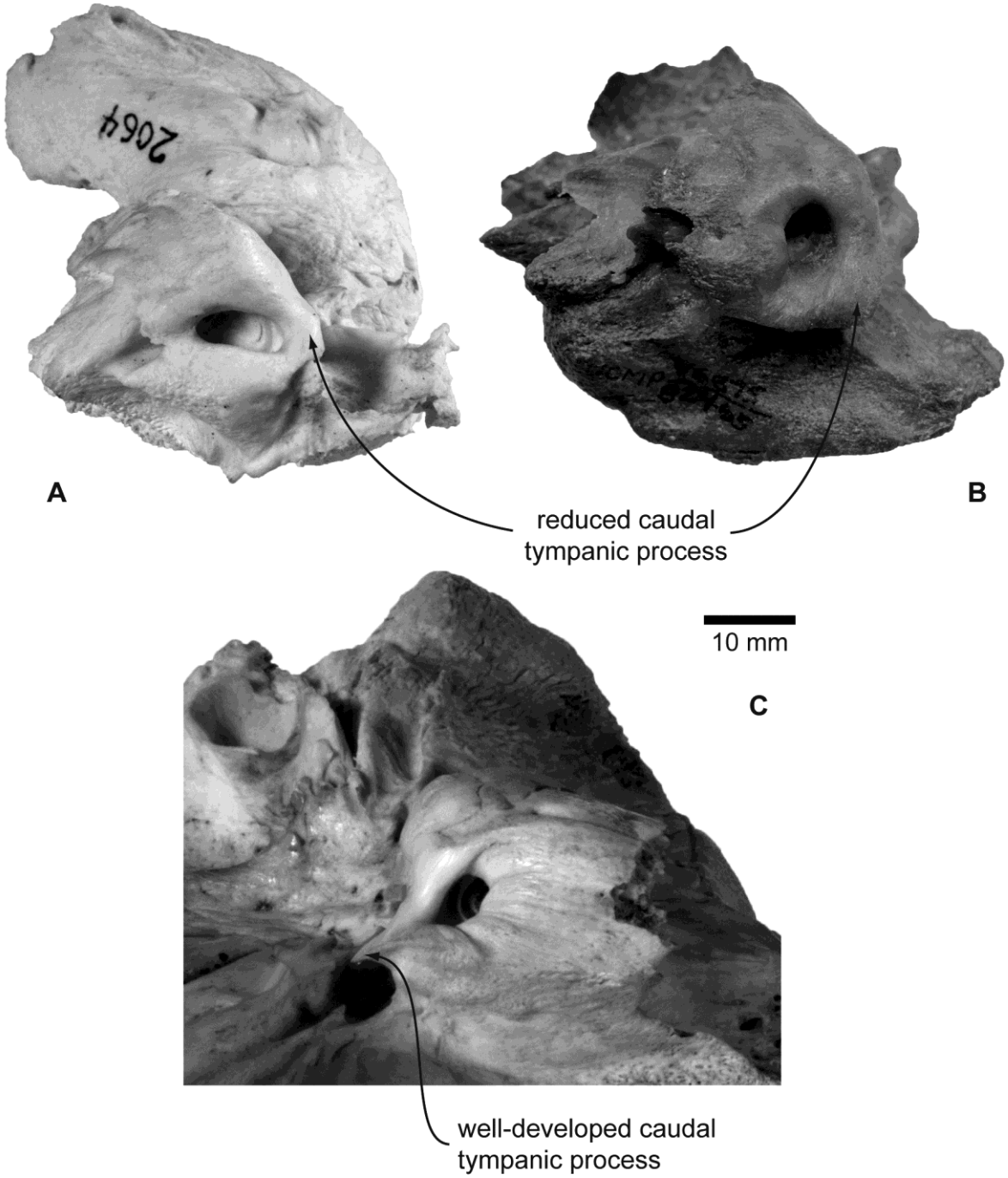

Figure S9 The pars cochlearis bearing the caudal tympanic process of (A) *Caperea marginata* (NMNZ MM002064), (B) *Herpetocetus bramblei* (UCMP 82465) and, (C) *Eubalaena australis* (OU, no number) in posteromedial view. All photographs are scaled to the same size.

S11). In *Caperea*, herpetocetines and balaenids in particular, this squared anterior end results in a rhomboid outline of the bulla, which has been suggested as a potential synapomorphy of a clade comprising *Caperea* and balaenids [13,14].

However, as shown here, a rhomboid outline of the bulla is not exclusive to those taxa, and could alternatively be interpreted as either a primitive character, or a feature which independently and convergently arose in balaenids and cetotheres (including *Caperea*), respectively.

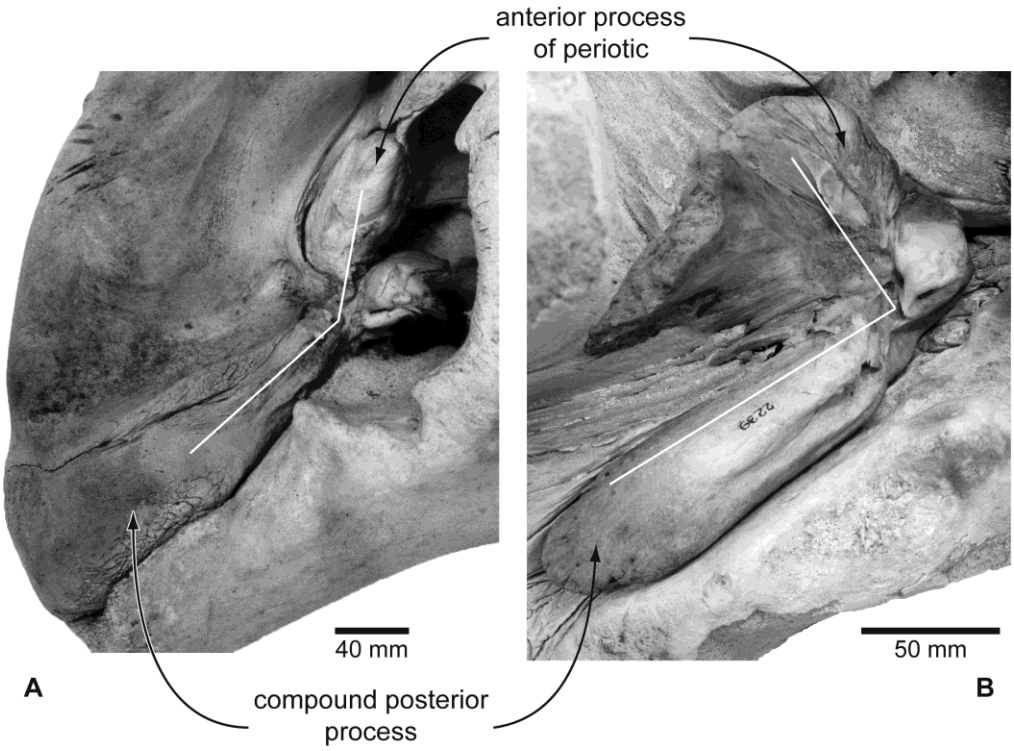

Figure S10 Ventral view of the articulated periotic showing the orientation of the compound posterior process in (A) *Caperea marginata* (OM VT227), and (B) *Eubalaena australis* (NMNZ MM002239).

Char. 113 Position of dorsal origin of lateral furrow: this character is based on the length of the anterior lobe of the tympanic bulla, previously defined as follows:

“The anterior lobe of the tympanic bulla is the ventral swelling of the bulla anterior to the sigmoid process. The length of the anterior lobe is measured as the greatest distance (perpendicular to the lateral furrow) from the base of the trough formed by the lateral furrow to the anteriormost point of the bulla.” [14:text S2, p.7]

In some taxa, such as *Eubalaena*, the determination of the length of the anterior lobe

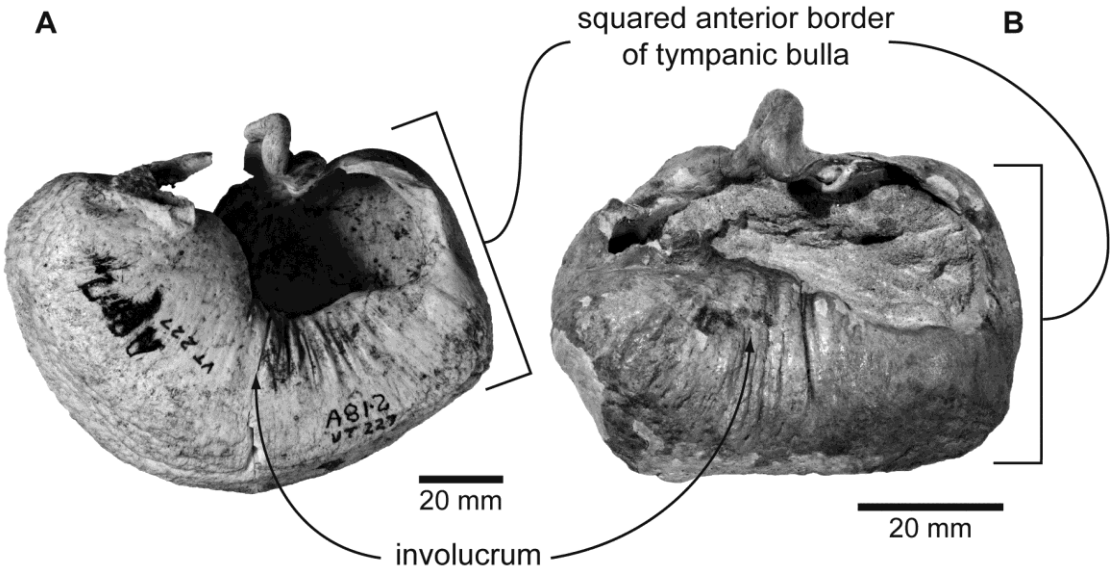

Figure S11 Dorsal view of the left tympanic bulla of (A) *Caperea marginata* (OM VT227), and (B) *Herpetocetus transatlanticus* (USNM 182962).

is made difficult by the presence of a strongly oblique, anteroventrally oriented lateral furrow, originating from the sigmoid process and terminating close to the anteromedial corner of the bulla. While the dorsalmost part of the lateral furrow in *Eubalaena* directly anterior to the sigmoid process is located roughly halfway along the total length of the bulla, its most ventral portion is located much closer to the anterior border of the latter. The length of the anterior lobe is therefore dependent on exactly where along the lateral furrow it is measured: the closer the point of measurement lies to the ventralmost part of the lateral furrow, the shorter the anterior lobe will seem.

For the sake of consistency, and following its original definition as “ventral swelling of the bulla anterior to the sigmoid process” [14], we therefore decided to measure the length of the anterior lobe with the bulla in lateral view, from the dorsalmost portion of the lateral furrow located directly anterior to the sigmoid process to the anterior border of the bulla (figure S12), and considered the anterior lobe to be short if the lateral furrow was positioned within the first third of the anteroposterior length of the bulla. Measured this way, the anterior lobe is markedly shorter than the posterior lobe in *Caperea*, herpetocetines, *Piscobalaena*, and *Balaena*, while being only slightly shorter or subequal to the posterior lobe in all other taxa included in this study.

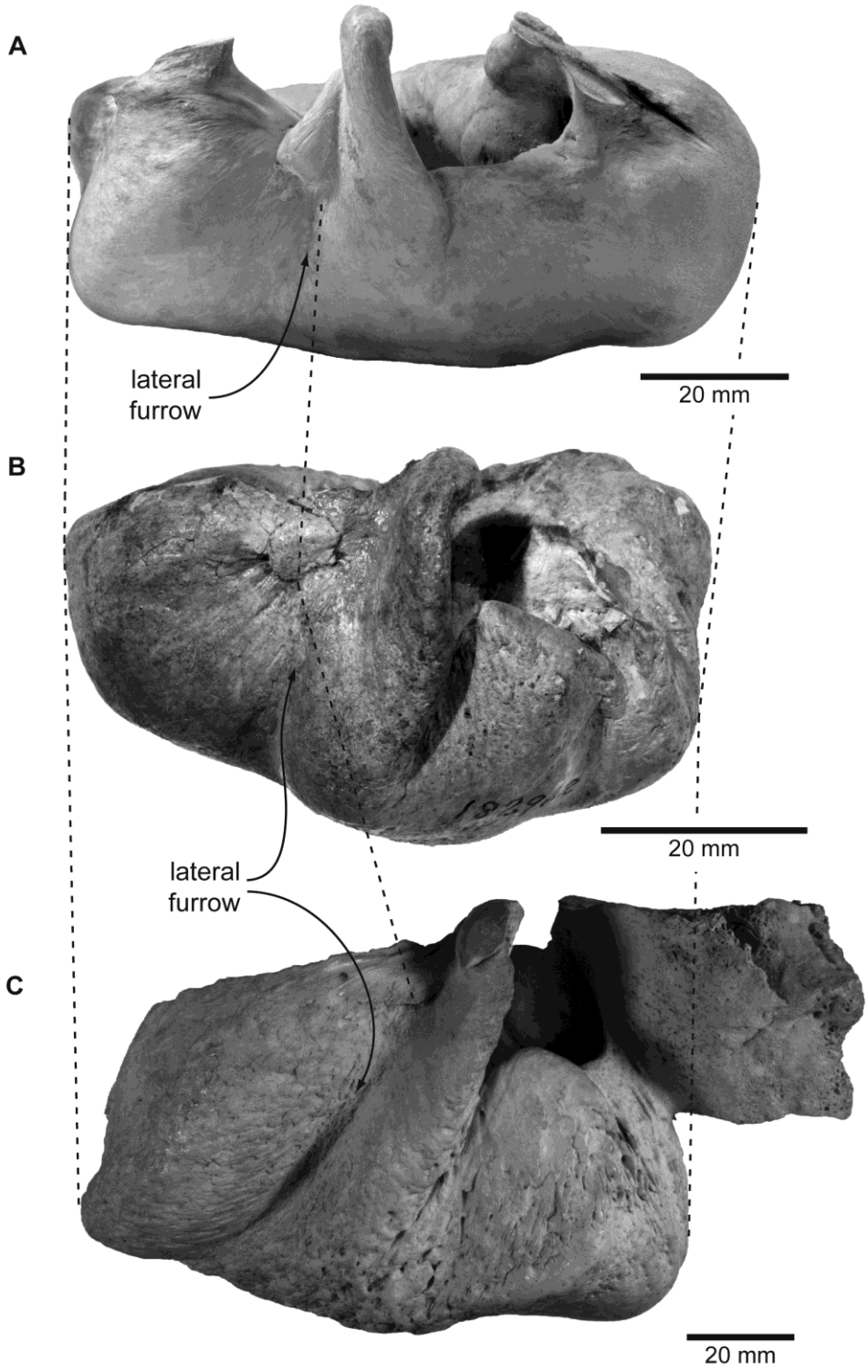

Figure S12 Lateral view of the tympanic bulla of (A) *Caperea marginata* (NMV C28531), (B) *Herpetocetus transatlanticus* (USNM 182962, length somewhat distorted as the photo was taken at a slight angle; see further illustrations on MorphoBank) and (C) *Eubalaena australis* (NMNZ MM000226). Note the strongly oblique lateral furrow of *Eubalaena australis*.

Char. 120 Shape of conical process in lateral view: in *Caperea*, herpetocetines, and some balaenids, including *Balaena mysticetus* and *Balaenula astensis*, the conical process of the tympanic bulla is poorly developed and represented by little more than a low ridge. By contrast, the conical process of virtually all other mysticetes is relatively tall and rounded in lateral view. A low conical process has been suggested as a potential synapomorphy of a clade comprising *Caperea* and balaenids [13,14]. However, the presence of this feature in herpetocetines demonstrates the wider distribution of this morphology, therefore allowing a different reconstruction of its evolutionary history.

Char. 131 Outline and position of tympanic sulcus: the tympanic sulcus is the site of attachment of the tympanic membrane or “glove finger” on the medial margin of the outer lip of the tympanic bulla [14,65]. The tympanic sulcus is developed as a nearly straight, horizontal crest, approaching or running through the point of intersection of the sigmoid and conical processes in *Caperea*, herpetocetines, and *Piscobalaena* (figure S13A,B). By contrast, in most other mysticetes the tympanic sulcus descends far below the point of intersection of the sigmoid and conical processes, following a semicircular path from the posterior pedicle of the bulla to the posterior border of the sigmoid process (figure S13C).

Char. 132 Anteroventral side of tympanic bulla: the ventral surface of the tympanic bulla of *Caperea* is transversely convex and well-rounded, with the exception of a variably developed, shallow groove running parallel to the posteromedial border of the bulla. This groove is restricted to the posterior half of the bulla and laterally offset from the main ridge, with the latter being broadly rounded. A concave ventral side of the bulla also occurs in balaenids. However, unlike in *Caperea*, the ventral surface of the bullae of balaenids is most strongly convex anteriorly. In addition, the concavity of the ventral surface in balaenids is not restricted to a groove, and instead broadly affects all of the anterior and part of the posterior portion of the tympanic bulla, resulting in a ventrally concave, “pinched” (i.e. dorsoventrally compressed) main ridge. In contrast to *Caperea* and balaenids, the ventral surface of the bulla of virtually all other mysticetes is transversely rounded.

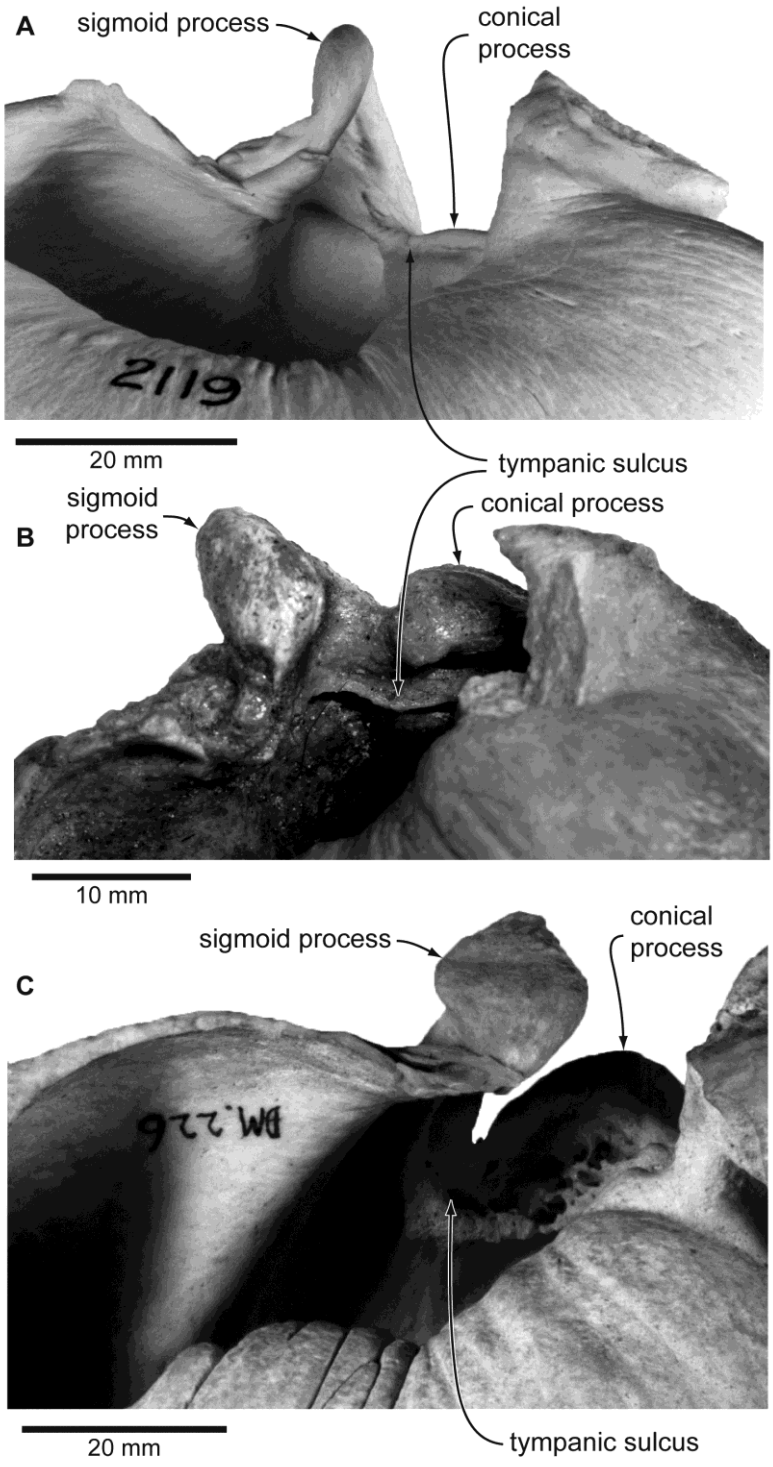

Figure S13 Tympanic sulcus of (A) *Caperea marginata* (NMNZ MM002119), (B) *Piscobalaena nana* (MNHN SAS892) and (C) *Eubalaena australis* (NMNZ MM000226) in dorsomedial view. Note the semicircular outline of the tympanic sulcus of *Eubalaena australis*.

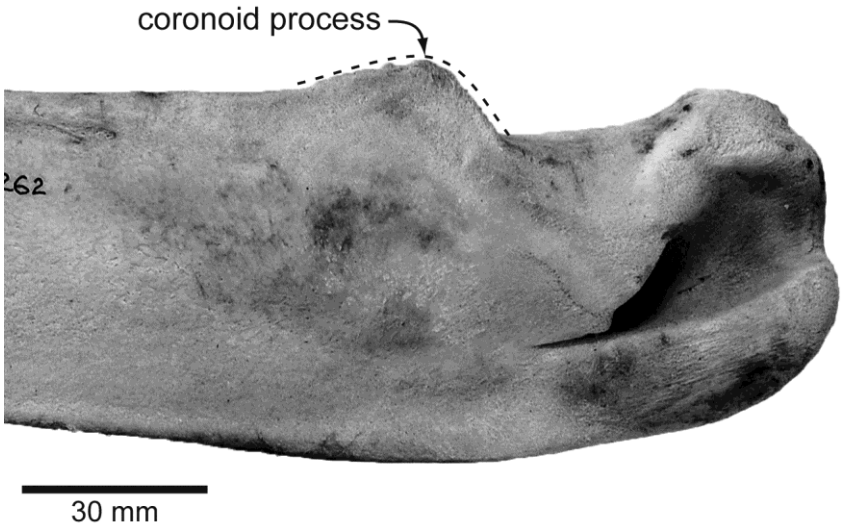

Figure S14 Posterior portion of the right mandible of a *Caperea marginata* neonate (NMNZ MM002262) in medial view. Note the bluntly triangular coronoid process.

Char. 145 Coronoid process in lateral or medial view: unlike adult specimens, juvenile *Caperea* retain a well-defined, bluntly triangular, and anteroposteriorly elongate coronoid process (figure S14). This resembles the condition found in *Piscobalaena*, herpetocetines [66], balaenids, and *Eschrichtius*, and contrasts with the higher and more sharply triangular coronoid process of balaenopterids and several extinct Miocene taxa, such as *Diorocetus* and *Pelocetus*.

Char. 148 Orientation of articular surface of mandibular condyle: the mandible of *Caperea* is highly autapomorphic compared to other mysticetes, with a highly arched horizontal ramus and a relatively small condyle. The articular surface of the latter is oriented roughly posterodorsally, in contrast to the more posteriorly oriented condyles of extant balaenopterids and the more dorsally directed condyles of balaenids and *Eschrichtius*. It should be noted that any accurate assessment of the orientation of the mandibular condyle in baleen-bearing mysticetes relies on the position of the mandibles themselves, which is unknown for most extinct taxa, and poorly described in many extant taxa, such as *Caperea* and balaenids, casting some doubt on the reliability of this character in cladistic analyses.

Char. 155 Shape of transverse processes of lumbar vertebrae: in most mysticetes, the transverse processes of the lumbar vertebrae are relatively slender and distinctly

wider transversely than long anteroposteriorly. By contrast, in *Caperea* and *Piscobalaena*, the transverse processes are longer anteroposteriorly and relatively narrower compared to other taxa, thus resembling a broad plate [7,67], although this might be an artifact of the greatly reduced number of lumbars in *Caperea*. The morphology of the transverse processes of herpetocetines is currently unknown.

5. Supplementary references

29. O'Leary, M. A. & Kaufman, S. G. 2007 MorphoBank 2.5: web application for morphological systematics and taxonomy; http://www.morphobank.org/
30. O'Leary, M. A. & Kaufman, S. G. 2011 MorphoBank: phylophenomics in the ''cloud''. *Cladistics* **27**, 529–537.
31. Goloboff, P. A., Farris, J. S. & Nixon, K. C. 2003 T.N.T.: tree analysis using new technology. Program and documentation available from the authors, and from www.zmuc.dk/public/phylogeny
32. Goloboff, P. A., Farris, J. S. & Nixon, K. C. 2008 TNT, a free program for phylogenetic analysis. *Cladistics* **24**, 774–786.
33. Huelsenbeck, J. P. & Ronquist, F. 2001 MRBAYES: Bayesian inference of phylogeny. *Bioinformatics* **17**, 754–755.
34. Ronquist, F. & Huelsenbeck, J. P. 2003 MRBAYES 3: Bayesian phylogenetic inference under mixed models. *Bioinformatics* **19**, 1572–1574.
35. Guindon, S., Gascuel O. A simple, fast, and accurate algorithm to estimate large phylogenies by maximum likelihood. *Syst. Biol.* **52**, 696–704 (2003).
36. Posada, D. 2008 jModelTest: Phylogenetic Model Averaging. *Mol. Biol. Evol.* **25**, 1253–1256.
37. Lewis, P. O. 2001 A likelihood approach for inferring phylogeny from discrete morphological characters. *Syst. Biol.* **50**, 913–925.
38. Nylander, J. A. A., Ronquist, F., Huelsenbeck, J. P. & Nieves-Aldrey, J. L. 2004 Bayesian phylogenetic analysis of combined data. *Syst. Biol*. **53**, 47–67.
39. Wiens, J. J., Bonett, R. M. & Chippindale, P. T. 2005 Ontogeny discombobulates phylogeny: paedomorphosis and higher-level salamander relationships. *Syst. Biol*. **54**, 91–110.

40. Kass, R. E. & Raftery, A. E. 1995 Bayes factors. *J. Am. Stat. Assoc*. **90**, 773–795.
41. Nylander, J. A. A., Wilgenbusch, J. C., Warren, D. L. & Swofford, D. L. 2008 AWTY (Are we there yet?): a system for graphical exploration of MCMC convergence in Bayesian phylogenetics. *Bioinformatics* **24**, 581–583.
42. Piller, W. E., Harzhauser, M. & Mandic, O. 2007 Miocene Central Paratethys stratigraphy – current status and future directions. *Stratigraphy* **4**, 151–168.
43. Vangengeim, E. A. & Tesakov, A. S. 2008 Late Sarmatian mammal localities of the eastern Paratethys: stratigraphic position, magnetochronology, and correlation with the European continental scale. *Strat. Geol. Correl.* **16**, 92–103.
44. Radionova, E. P. *et al.* 2012 Middle-Upper Miocene stratigraphy of the Taman Peninsula, Eastern Paratethys. *Cent. Eur. J. Geosci*. **4**, 188–204.
45. Cope, E. D. 1896 Sixth contribution to the knowledge of the Miocene fauna of North Carolina. *Proc. Am. Phil. Soc.* **35**,139–146.
46. Kellogg, R. 1968 Miocene Calvert mysticetes described by Cope. *Bull. U. S. Natl. Mus*. **247**, 103–132.
47. Case, E. C. 1904 Mammalia. In *Miocene (Text)* (eds. W. B. Clark, G. B. Shattuck & W. H. Dall), pp. 3–58. Baltimore: Maryland Geological Survey.
48. Ward, L. W. & Powars, D. S. 2004 Tertiary lithology and paleontology, Chesapeake Bay region *U. S. Geol. Surv. Circ.* **1264**, 163–297.
49. Wijnker, E. & Olson, S. L. 2009 A revision of the fossil genus *Miocepphus* and other Miocene Alcidae (Aves: Charadriiformes) of the western North Atlantic Ocean. *J. Syst Palaeontol.* **7**, 471–487.
50. Petuch, E. J. & Drolshagen, M. 2010 *Molluscan Paleontology of the Chesapeake Miocene.* Boca Raton: CRC Press, Boca Raton.
51. Scasso, R. A., Castro, L. N. 1999 Cenozoic phosphatic deposits in North Patagonia, Argentina: phosphogenesis, sequence-stratigraphy and paleoceanography. *J. S. Am. Earth Sci.* **12**, 471-487.
52. Cione, A. L., Cozzuoal, M. A., Dozo, M. T., Hospitaleche, C. A. 2011 Marine vertebrate assemblages in the southwest Atlantic during the Miocene. *Biol. J. Linn. Soc.* **103**, 423-440.
53. Dunn, R. E., Kohn, M. J., Madden, R. H., Strömberg, C. E.; Carlini, A. A. 2009 High Precision U/Pb Geochronology of Eocene-Miocene South American

Land Mammal Ages at Gran Barranca, Argentina. Abstract #GP23B-0791, American Geophysical Union, Fall Meeting 2009.

54. Kellogg, R. 1929 A new cetothere from southern California. *Univ. Calif. Publ. Geol. Sci*. **18**, 449–457.
55. Beyer, L. A. *et al.* 2009 Post-Miocene Right Separation on the San Gabriel and Vasquez Creek Faults, with Supporting Chronostratigraphy, Western San Gabriel Mountains, California. *U.S. Geol. Surv. Prof. Paper* **1759**, 1–44.
56. Repenning, C.A. Tedford, R. H. 1977 Otarioid seals of the Neogene. *U. S. Geol. Surv. Prof. Pap.* **992**, 1–93.
57. Prothero, D. R. 2001 Chronostratigraphic calibration of the Pacific coast Cenozoic: a summary. In *Magnetic Stratigraphy of the Pacific Coast Cenozoic*. (ed. D. R. Prothero), *Pacific Section*. *SEPM Book* **91**, 377–394 (2001).
58. Ehret, D. J., MacFadden, B. J., Jones, D. S., DeVries, T. J., Foster, D. A. & Salas-Gismondi, R. 2012. Origin of the white shark Carcharodon (Lamniformes: Lamnidae) based on recalibration of the Upper Neogene Pisco Formation of Peru. *Palaeontology* **55**, 1139–1153.
59. Muizon, C. de, & DeVries, T. J. 1985 Geology and paleontology of late Cenozoic marine deposits in the Sacaco area (Peru). *Geol. Rundschau* **74**, 547–563.
60. True, F. 1904 The whalebone whales of the western North Atlantic. *Smithsonian Contrib. Knowl.* **33**, 1–332.
61. Van Beneden, P.-J. Gervais, P. 1868–1879 *Ostéographie des cétacés vivant et fossiles*. Paris: Arthus Bertrand.
62. De Pinna, M. G. G. 1991 Concepts and tests of homology in the cladistic paradigm. *Cladistics* **7**, 367–394.
63. Rieppel, O. & Kearney, M. 2002 Similarity. *Biol. J. Linn. Soc. Lond.* **75**, 59–82.
64. Agnarsson, I. & Coddington, J. A. 2008 Quantitative tests of primary homology. *Cladistics* **24**, 51-61.
65. Fraser, F. C. & Purves, P. E. 1960 Hearing in Cetaceans. *B. Brit. Mus. (Nat. Hist.) Zool.* **7**, 1–140.
66. Boessenecker, R. W. 2011 Herpetocetine (Cetacea: Mysticeti) dentaries from the Upper Miocene Santa Margarita Sandstone of Central California. *PaleoBios* **30**, 1–12.

67. Buchholtz, E. A. 2011 Vertebral and rib anatomy in *Caperea marginata*: Implications for evolutionary patterning of the mammalian vertebral column. *Mar. Mamm. Sci.* **27**, 382–397.

6. Branch support

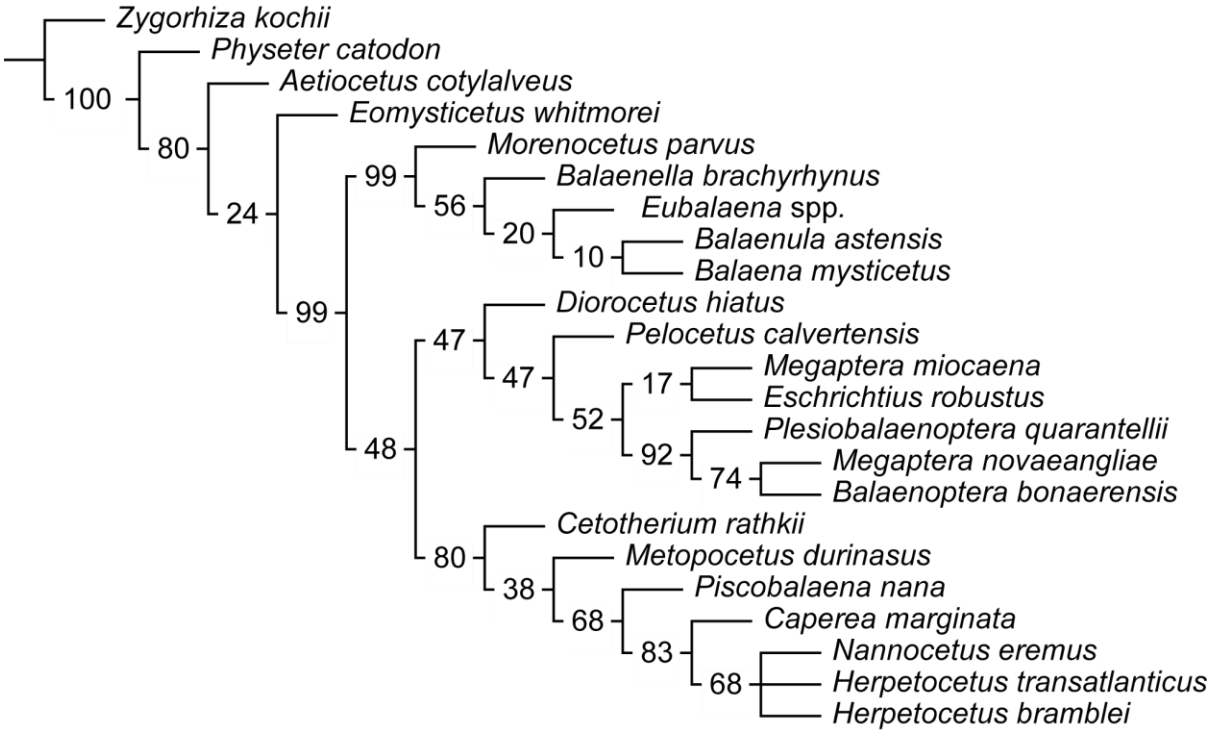

Figure S15 Symmetric resampling, shown as GC values [27] arising from the parsimony-based analysis of the morphological data only

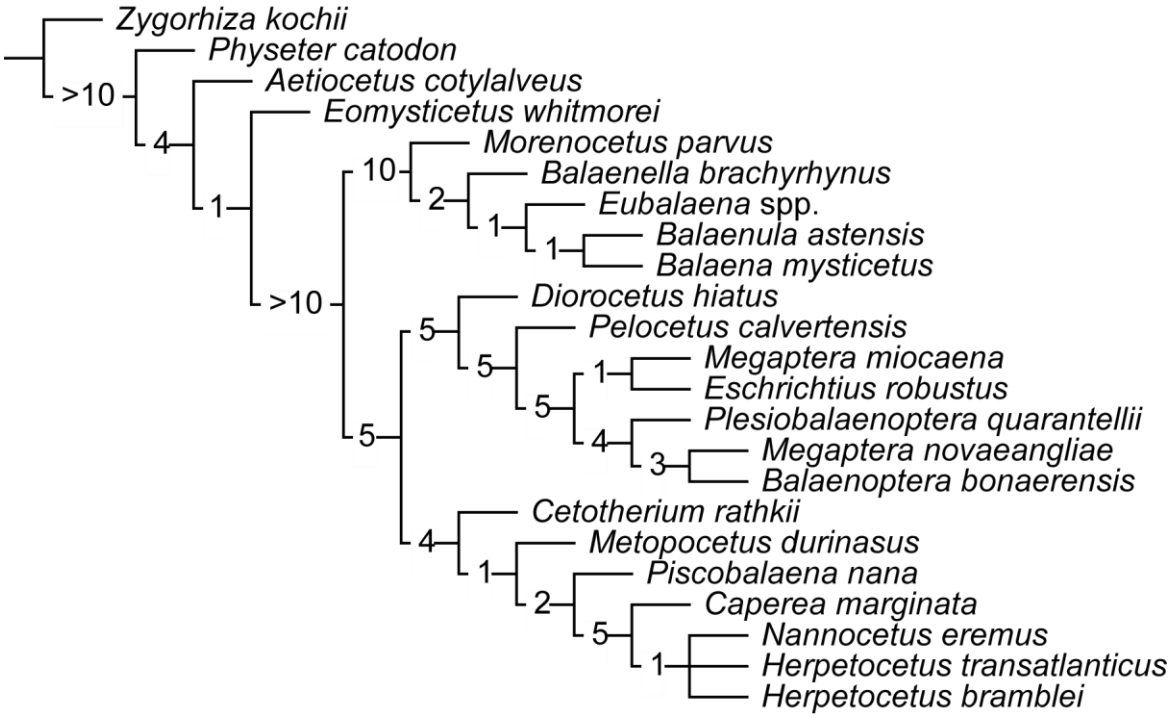

Figure S16 Bremer decay values [26] arising from the parsimony-based analysis of the morphological data only

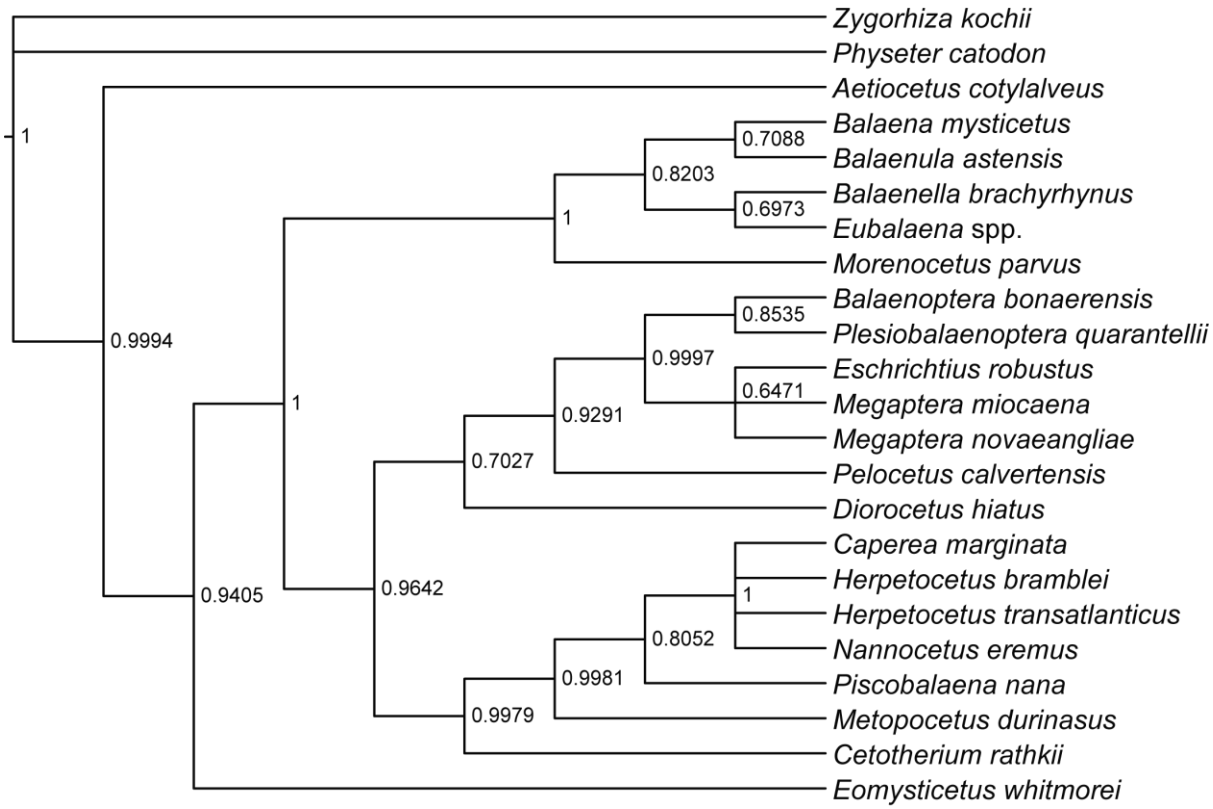

Figure S17 Bayesian posterior probabilities arising from the total evidence analysis of the combined molecular and morphological data.

7. Institutional Abbreviations

ALMNH, Alabama Museum of Natural History, Tuscaloosa, USA; **AMP**, Ashoro Museum of Paleontology, Ashoro, Hokkaido, Japan; **ChM**, The Charleston Museum, Charleston, USA; **FMNH**, The Field Museum of Natural History, Chicago, USA; IRSNB, Institute Royal des Sciences Naturelles, Bruxelles, Belgium; **LACM**, Natural History Museum of Los Angeles County, Los Angeles, USA; **MLP**, Museo de La Plata, La Plata, Argentina; **MNHN**, Museum National d`Histoire Naturelle, Paris, France; **MPST**, Museo Paleontologico di Salsomaggiore Terme, Salsomaggiore Terme, Italy; **MSNTUP**, Museo di Storia Naturale e del Territorio, Università di Pisa, Pisa, Italy; **NHMUK**, The Natural History Museum, London, United Kingdom; **NMB**, Natuurmuseum Brabant, Tilburg, The Netherlands; **NMNS**, National Museum of Nature and Science, Tokyo, Japan; **NMNZ**, Museum of New Zealand Te Papa Tongarewa, Wellington, New Zealand; **NMV**, Museum Victoria, Melbourne, Australia; **NMV**, National Museum of Wales Amgueddfa Cymru, Cardiff, Wales, United Kingdom; **OM**, Otago Museum, Dunedin, New Zealand; **OU**, Geology Museum, University of Otago, Dunedin, New Zealand; **PIN**, Paleontological Institute, Moscow, Russia; **SBAER**, Soprintendenza per i Beni Archeologici dell'Emilia Romagna; **SMNK**, Staatliches Museum für Naturkunde, Karlsruhe, Germany; **UCMP**, University of California Museum of Paleontology, Berkeley, USA; **USNM**, United States National Museum of Natural History, Washington DC, USA;

8. List of studied material

Outgroup:

Zygorhiza kochii: ALMNH 2000.1.2.1; USNM 11962; photos of USNM 4678, 4679, 12063, 16438, 16639, 537887 provided by M. Uhen; *Zygorhiza* sp. OU 22100, 22222-1, 22242;
Physeter macrocephalus: MSNTUP M266; NMNS M24821, M32579, M34048; USNM 253051;

Ingroup:

Aetiocetus cotylalveus: USNM 25210; photos of USNM 25210 provided by E. Fitzgerald;
Balaena mysticetus: NMNS M25893; USNM 15695, 63301; photos of IRSNB 1532 provided by Mark Bosselaers; photos of LACM 54479 provided by Dave Janiger; photos of NHMUK 1934.10.10.1 provided by Jerry Hooker; photos of USNM 63300 obtained from [14];

Balaenella brachyrhynus: NMB 42001;
Balaenoptera bonaerensis: NMNS M19792, M24357; OM VT3057, VT3060;
Balaenula astensis: MSNTUP I12555;
Caperea marginata: NMNZ MM002064, MM002119, MM002898, MM002235, MM002900, MM002254, MM002262, MM002232; NMV C28531; OM VT227;
Cetotherium rathkii: photos of PIN 1840/1 provided by Pavel Gol'din, Mette Steeman and Constantine Tarasenko;
Diorocetus hiatus: USNM 16783, 23494;
Eomysticetus whitmorei: ChM PV4253; photos of ChM PV4253 provided by A. Sanders;
Eschrichtius robustus: AMP R09; NMNS M25899; USNM 13803, 364973, 364975; photos of USNM 13803 provided by E. Fitzgerald and downloaded from the USNM collection records (http://collections.mnh.si.edu/search/mammals/);
Eubalaena spp. (*E. glacialis*): FMNH 15559; MSNTUP M264; USNM A23077, 505886; photos downloaded from the USNM collection records (http://collections.mnh.si.edu/search/mammals/);
Eubalaena spp. (*E. australis*): NMNZ MM000226, MM002239; NMV C28603; OU, no number; USNM 267612;
Herpetocetus bramblei: UCMP 82465;
Herpetocetus transatlanticus: USNM 182962;
"*Megaptera*" *miocaena*: USNM 10300;
Megaptera novaeangliae: NMNS M33734; NMNZ MM000228; NMW Z.1982.058; photos of MSNTUP M263 provided by C. Sorbini and G. Bianucci; photos of USNM 13656, 301636 downloaded from the USNM collection records (http://collections.mnh.si.edu/search/mammals/);
Metopocetus durinasus: USNM 8518; photos of
Morenocetus parvus: photos of MLP 5-11 provided by M. Buono;
Nannocetus eremus: UCMP 26502;
Pelocetus calvertensis: USNM 11976;
Piscobalaena nana: MNHN SAS 892, SAS1616, SAS1617, SAS1618; SMNK Pal4050;
Plesiobalaenoptera quarantellii: MPST/ SBAER 240505;

9. Character list

Details on the previous use of individual characters are provided as part of MorphoBank project 578 (www.morphobank.org).

Cranium (excluding tympanoperiotic)

1. Length of rostral portion of maxilla: less than bizygomatic width (0); equal to or greater than bizygomatic width (1).

2. Lateral border of maxilla anterior to antorbital notch or homologous point on rostrum in dorsal view: concave (0); straight (1); broadly convex (2).

3. Transverse width of maxillae at midpoint: distinctly less than that of the premaxillae (0); roughly equal to or greater than that of the premaxillae (1).

4. Premaxilla in dorsal view: portion anterior to nasal opening narrows or remains the same width anteriorly (0); widens at anterior end (1).

5. Abrupt increase in dorsoventral height of premaxilla adjacent to anterolateral corner of nasal: absent (0); present (1).

6. Premaxilla on central part of rostrum in lateral view: convex and elevated above the maxilla and forming a distinct lateral face (0); flattened and continuous or nearly continuous with the maxilla (1).

7. Premaxillae adjacent to and at posterior edge of nasal opening: do not clearly overhang maxillae (0); premaxillae overhang maxillae (1).

8. Medial contact of premaxillae in dorsal view: contact anteriorly along midline (0); separated along the entire length of the rostrum (1).

9. Antorbital process: absent (0); present and defined by a steep face clearly separating the posterolateral corner of the maxilla from the more clearly separating the posterolateral corner of the maxilla from its more anterior rostral portion (1); present as a distinct anterior projection lateral to antorbital notch (2).

10. Posterolateral corner of maxilla and anterior border of supraorbital process of frontal in dorsal view: maxilla closely approximates or underlies frontal (0); separated by a basin distinct from the space for the reception of the lacrimal (1); maxilla overrides anteriormost border of supraorbital process of frontal (2).

11. Distinct pocket between the ascending process of the maxilla dorsally and the supraorbital process ventrally: absent (0); present (1).

12. Posterior end of ascending process of premaxilla: no contact with frontals (0); contact frontals with their posteriormost tips only (1); form robust contact with frontals (2).

13. Lateral borders of ascending process of maxilla: lateral edges convergent with the process tapering to a point (0); lateral edges parallel or divergent posteriorly (1).

14. Lateral process of maxilla: absent (0); present and forming an antorbital notch in dorsal view (1).

15. Posterior portion of palatal surface of maxilla: palate is flat or slightly concave (0); sagittal portion of maxilla forms a longitudinal keel bordered laterally by shallow longitudinal troughs (1); sagittal portion forms a keel but without adjacent troughs (2).

16. Palatal surface of anterior part of rostrum: flat or gently concave (0); bears pronounced longitudinal keel formed by vomer and medial edges of maxillae along the midline of the rostrum (1).

17. Exposure of premaxilla on palate: present and exposed along at least one third of the length of the maxilla (0); limited in extent to less than one third the length of the maxilla (1).

18. Palatal window exposing vomer: absent (0); present (1); narrow and variable exposure of vomer along most or all the midline of the rostrum (2); vomer broadly exposed along most or all of the midline of the rostrum (3).

19. Palatal nutrient foramina and sulci: absent (0); present (1).

20. Outline of suture between maxillae and palatines: roughly straight transversely or bowed anteriorly (0); forms a posteriorly pointing V shape (1); anterior margins of palatines form two separate and posteriorly pointing U shapes (2).

21. Outline of rostrum in lateral view: portion anterior to the nasals is abruptly depressed (0); transition from the anterior end of the rostrum to the nasals is smooth (1).

22. Teeth in adult individuals: present (0); absent or vestigial (1).

23. Anterior edge of supraorbital process lateral to ascending process of maxilla: oriented transversely or pointing anteriorly (0); pointing posteriorly (1); linguiform and tapering to a point (2).

24. Posterior border of supraorbital process in dorsal view: concave (0); straight (1).

25. Supraorbital process of frontal: horizontal (0); gradually slopes away lateroventrally from the skull vertex (1); abruptly depressed to a level noticeably below the vertex with the lateral skull wall above the supraorbital formed by both

parietal and frontal (2); as state 2 but with the lateral skull wall above the supraorbital formed by parietal only (3).

26. Width of supraorbital process as measured in a straight line along posterior border: equal to or shorter than the anteroposterior length of the supraorbital process above the orbit (0); up to twice the length above orbit (1); more than twice the length above orbit (2).

27. Position of anteriormost point of supraorbital process: in line with the posterior extremity of the nasals or passing through the nasals (0); on the same level as the anterior extremity of the nasals (1); anterior to the anterior extremity of the nasals (2).

28. Dorsal edge of orbit relative to lateral edge of rostrum with skull resting on a horizontal surface: elevated above the lateral edge of the rostrum (0); roughly in line with the lateral edge of the rostrum (1); located well below the lateral edge of the rostrum (2).

29. Contact of jugal with zygomatic process of the squamosal: the two bones overlap dorsoventrally (0); little or no overlap (1).

30. Maxillary infraorbital plate: absent (0); present (1).

31. Maxillary window originating from posterior border of infraorbital plate: absent (0); present (1).

32. Anteromedial corner of supraorbital process of frontal extending to a point medial to antorbital notch: absent (0); present (1).

33. Position of posteriormost edge of ascending process of maxilla: in transverse line with anterior half or halfway point of supraorbital process (0); in line with posterior half of supraorbital process or postorbital process (1); extends to a point posterior to the postorbital process (2).

34. Posterior ends of ascending processes of maxillae in dorsal view: widely separated by either frontals or both nasals and premaxillae (0); posterior processes are converging towards the midline and are either separated by the nasals only or contact along the midline (1).

35. Relative position of posteriormost edge of ascending process of maxilla in dorsal view: approximately in transverse line with or posterior to posterior edge of nasal (0); anterior to posterior edge of nasal (1).

36. Length of nasals relative to bizygomatic width: between 25 and 50% of bizygomatic width (0); less than 25% of bizygomatic width (1); more than 50% of bizygomatic width (2).

37. Posterior portion of nasals: blocky or triangular with medially converging lateral borders (0); strongly compressed into a transversely thin and barely visible sheet of bone (1).

38. Anterior margins of nasals: roughly straight or U-shaped (0); form a distinct and posteriorly pointing W shape (1); with point on midline and a gap on each side between premaxilla and nasal (2).

39. Dorsal surface of nasals: flattened (0); developed into a sagittal keel (1).

40. Separation of posterior portions of nasals along sagittal plane by narial process of frontals: present (0); absent (1).

41. Position of posteriormost edge of nasals: in transverse line with anterior half or halfway point of supraorbital process of frontal (0); in line with posterior half of supraorbital process (1); located posterior to or in line with posteriormost edge of postorbital process (2).

42. Zygomatic process of squamosal and exoccipital in dorsal view: clearly separated by an angle (0); posterior border of zygomatic process and lateral edge of exoccipital are confluent forming a continuous or nearly continuous lateral skull border (1).

43. Orbitotemporal crest: positioned along posterior border of supraorbital process with origin of temporal muscle facing posteriorly or posteroventrally (0); absent or positioned on dorsal surface of supraorbital process with origin of temporal muscle facing posterodorsally or dorsally (1).

44. Area enclosed by orbitotemporal crest on supraorbital process of frontal: restricted to posteromedial quarter of supraorbital process (0); distinctly U-shaped and extending almost to anterior border of supraorbital process (1); covering half or more of the dorsal surface of supraorbital process and almost reaching its posterolateral corner (2).

45. Shape of temporal fossa: longer anteroposteriorly than wide transversely or as wide as long (0); wider than long (1).

46. Intertemporal constriction: longer anteroposteriorly than wide transversely (0); as state 1 with the temporal fossa forming a large parasagittal oval (1); wider transversely than long anteroposteriorly (2).

47. Parietal and interparietal: anteriormost point located no further forward than postorbital process (0); anteriormost point in line with supraorbital process (1).

48. Parietals in lateral view: as long or longer anteroposteriorly than high dorsoventrally (0); higher dorsoventrally than long anteroposteriorly (1).

49. Anteriormost point of parietal and interparietal: more posterior than posterior border of the ascending process of the maxilla (0); more anterior than or in line with posterior border of the ascending process of the maxilla (1).

50. Anteriormost point of supraoccipital in dorsal view: located posterior to or in line with the level of the anterior end of the zygomatic process of the squamosal (0); located anterior to the level of the anterior end of the zygomatic process of the squamosal (1); in line with the anterior half or anterior edge of the supraorbital process (2).

51. Anteroposterior position of posterior apex of nuchal crest: posterior to the condyles (0); anterior to or in line with the posteriormost point of the occipital condyles (1).

52. Distinct nuchal tubercle at junction of parieto-squamosal suture and supraoccipital: absent (0); present (1).

53. Exposure of alisphenoid in temporal fossa: exposed on temporal wall of skull and contributing to orbital fissure (0); as state 0 but with alisphenoid broadly exposed and forming the ventral border of a large foramen also enclosed by the squamosal and parietal (1); exposed on temporal wall of skull but not contributing to orbital fissure (2); not exposed on temporal wall of skull (3).

54. Orientation of zygomatic process of squamosal: directed anteromedially (0); directed anteriorly (1); directed anterolaterally (2).

55. Zygomatic process of squamosal in lateral view: dorsal and ventral borders parallel or convergent anteriorly (0); process is expanded dorsoventrally both anteriorly and posteriorly, thus forming a medial constriction (1).

56. Anterior tip of zygomatic process of squamosal: situated entirely posterior to the postorbital process (0); closely apposed to the postorbital process or situated ventral to the latter (1).

57. Supramastoid crest of zygomatic process of squamosal: present (0); absent (1).

58. Size of squamosal including zygomatic and postglenoid processes: longer anteroposteriorly than high dorsoventrally or about as high as long (0); distinctly higher than long (1).

59. Parieto-squamosal suture shaped like a crest or ridge: absent (0); present (1).

60. Squamosal prominence: forms a projection on the crest delimiting the lateral or posterolateral edge of the squamosal fossa (0); absent (1).

61. Transverse width of squamosal lateral to exoccipital width: equal to or greater than 15% of the distance between the sagittal plane and the lateral edge of the exoccipital (0); exposed portion of squamosal is less than 15% of that distance (1).

62. Length of squamosal fossa relative to maximum transverse width of temporal fossa as measured in a straight line from the posteriormost point of the subtemporal crest to the posteriormost point of the nuchal crest: length of squamosal fossa is equal to or exceeds the width of the temporal fossa (0); length of squamosal fossa is three quarters the width of the temporal fossa or longer (1); length squamosal fossa is less than three quarters the width of the temporal fossa (2).

63. Postglenoid process in lateral view: ventral tip is curving anteriorly (0); anterior and posterior sides nearly parallel with the tip of the process pointing ventrally (1); as state 1 but with the tip of the process pointing posteriorly (2); process is triangular in outline with the tip pointing posteriorly or ventrally (3); process is triangular with the anterior border descending posteroventrally and the posterior border descending anteroventrally (4).

64. Ventral extension of postglenoid process in lateral view: ventral edge of postglenoid process approximately in line with or dorsal to ventral edge of exoccipital (0); extending well ventral to the ventral edge of the exoccipital (1).

65. Orientation of postglenoid process in posterior view: ventrally oriented (0); ventrolaterally oriented (1); ventromedially oriented (2).

66. Outline of postglenoid process in anterior or posterior view: parabolic (0); as state 0 but with lateral and medial edges parallel or concave (1); triangular (2); trapezoidal with a ventrally directed medial border (3).

67. Twisting of postglenoid process in ventral view: not twisted and roughly transverse to the sagittal axis of the skull (0); twisted clockwise on the left side and anticlockwise on the right side (1).

68. Squamosal cleft: absent (0); present (1).

69. Lateral edges of supraoccipital in dorsal view: convex (0); straight or concave (1).

70. Sagittal crest on supraoccipital shield: absent or indistinct (0); restricted to anterior half of supraoccipital shield (1); restricted to a depression in the center of the supraoccipital shield (2); present and running all the way along the supraoccipital shield (3).

71. Pterygoids in ventral view: pterygoids partially or entirely exposed (0); palatines almost completely cover pterygoids and extend on to the hamular process (1).

72. Pterygoid sinus fossa: extended anterior to foramen ovale or pseudovale (0); anterior edge approximately in line with or posterior to anterior edge of foramen ovale or pseudovale (1).

73. Superior lamina of pterygoid: absent or forming less than half of the roof of the pterygoid fossa (0); present and covering most of the ventral exposure of the alisphenoid (1).

74. Shape of pterygoid hamuli: shaped like a finger (0); expanded into a dorsoventrally flattened plate partially flooring the pterygoid sinus fossa (1); reduced in size or almost absent (2).

75. Position of foramen pseudovale (= external foramen ovale): foramen located within squamosal or between squamosal and pterygoid and opening anterolaterally or laterally (0); as state 0 but with foramen opening posteriorly (1); foramen lies within pterygoid (2).

76. Fossa on squamosal for reception of sigmoid process tympanic bulla: present (0); absent (1).

77. Base of postglenoid process in ventral view: in line with the center of the tympanic bulla (0); in line with the anterior half of the tympanic bulla or anterior to the latter (1); posterior to the anteroposterior center of the tympanic bulla (2).

78. Ventral border of sagittal part of vomer in ventral view: posteriormost portion projects beyond the posterior border of the palatines and is visible in ventral view (0); completely covered by palatines (1).

79. Basioccipital crest: narrow transversely (0); wide and bulbous (1).

80. Angle formed by the basioccipital crests in ventral view: diverging posteriorly (0); parallel or sub-parallel with no angle formed (1).

81. Posteriormost point of exoccipital in dorsal or ventral view: extends anterior to the posterior edge of occipital condyle (0); level with or posterior to posterior edge of condyle (1).

Hyoid apparatus

82. Outline of stylohyal in cross section: cylindrical (0); flattened (1).

83. Ankylosed basihyal and thyrohyals: absent (0); present (1).

Periotic

84. Dorsal and medial elongation of pars cochlearis towards cranial cavity: absent (0); present (1); present but with only the anterior side of the pars cochlearis being elongated (2).

85. Anterior process in lateral view: rounded or squared off (0); pointed and tapering (1); anterior border of process is strongly concave and shaped like an L (2).

86. Ventral edge of anterior process in medial view: at same level or dorsal to ventral edge of pars cochlearis (0); ventral to ventral profile of the pars cochlearis (1).

87. Length of anterior process as measured from the anterior border of the pars cochlearis: shorter than the anteroposterior length of the pars cochlearis (0); approximately same length or longer than the pars cochlearis (1).

88. Attachment of anterior process to pars cochlearis in taxa with a cranially elongated pars cochlearis: absent (0); present (1).

89. Anteroexternal sulcus: forms an oblique or vertical groove on lateral side of anterior process immediately anterior to lateral tuberosity (0); absent (1).

90. Dorsal junction between pars cochlearis and suprameatal area extended dorsally as a robust pyramidal process: absent (0); present (1).

91. Articulation of anterior process of periotic and tympanic bulla: no contact or contact with accessory ossicle via fovea epitubaria on the anterior process of the periotic (0); accessory ossicle or homologous region on periotic fused to bulla (1).

92. Lateral tuberosity of anterior process: absent or blunt and bulbous projection (0); hypertrophied (1); developed as a broad and anterolaterally pointing shelf articulating with the squamosal (2).

93. Distinct ridge delimiting insertion surface of tensor tympani on medial side of anterior process: absent (0); absent but insertion surface distinctly excavated (1); present (2).

94. Anteromedial corner of pars cochlearis in ventral view: angular and projecting medially resulting in a flattened ventral surface of the pars cochlearis (0); smooth and rounded (1).

95. Promontorial groove on medial side of pars cochlearis: present (0); present and deeply excavated (1); absent (2).

96. Caudal tympanic process of periotic in posteromedial view: well separated from crista parotica (0); narrow separation or contact (1).

97. Posteromedial corner of pars cochlearis medial to fenestra rotunda: rounded and level with fenestra rotunda (0); inflated and projecting posteriorly beyond fenestra rotunda (1).

98. Morphology of caudal tympanic process: absent or poorly developed (0); developed as a posteriorly extending triangular shelf (1); developed as a robust and ventrally directed projection (2).

99. Anteroposterior alignment of proximal opening of facial canal, internal acoustic meatus and aperture for cochlear aqueduct: present (0); absent (1).

100. Anteroposterior alignment of aperture for cochlear aqueduct and aperture for vestibular aqueduct: absent (0); present (1).

101. Prominent septum dividing foramina for vestibular and cochlear nerves within internal acoustic meatus: present (0); absent (1).

102. Size of aperture for cochlear aqueduct: smaller than aperture for vestibular aqueduct (0); approximately the same size (1).

103. Superior process: present as a distinct crest forming the lateral wall of the suprameatal fossa (0); the lateral border of the suprameatal fossa is low and rounded or not clearly defined (1).

104. Development of crista transversa: depressed well below the rim of the meatus (0); well developed and reaching the cerebral surface of the pars cochlearis (1).

105. Morphology of proximal opening of facial canal: roughly circular (0); anterior border is continuous with hiatus Fallopii and shaped like a fissure (1).

106. Size of proximal opening of facial canal: no more than half the size of the internal acoustic meatus (0); more than half the size of the internal acoustic meatus (1).

107. Articulation surfaces on posterior processes of tympanic bulla and periotic: unfused (0); fused in adults (1).

108. Morphology of facial sulcus on distal half of compound posterior process: absent or relatively shallow sulcus with equally defined anterior and posterior borders (0); marked groove with an elevated anterior border (1); deeply incised and partially floored tubular canal (2).

109. Orientation of compound posterior process in ventral view with periotic being *in situ*: oriented posterolaterally with respect to the longitudinal axis of the anterior process of the periotic (0); oriented at a right angle to the axis of the anterior process (1).

110. Shape of compound posterior process: cylindrical or slightly conical (0); flattened (1); forms a distinct plug (2).

111. Exposure of compound posterior process on lateral skull wall: external surface of posterior process is small or not clearly defined (0); process terminates in a distinct distal surface forming part of the lateral wall of the skull (1).

Tympanic bulla

112. Anterior border of bulla in dorsal or ventral view: pointed or rounded (0); squared (1).

113. Position of dorsal origin of lateral furrow: located along the posterior two thirds of the anteroposterior length of the bulla (0); located at roughly one third of the anteroposterior length of the bulla (1).

114. Orientation of lateral furrow: oriented ventrally (1); points distinctly anteroventrally (2);

115. Orientation of ventral keel or main ridge of lateral lobe of bulla: faces ventrally (0); faces ventromedially or medially (1).

116. Outline of lateral lobe or main ridge of bulla: concave (0); straight or convex (1).

117. Involucral ridge in dorsal view: involucral ridge coincident with medial edge irrespective of the degree of rotation of the bulla (0); involucral ridge laterally retracted (1).

118. Dorsomedial corner of sigmoid process in anterior view: separated from the pedicle of the malleus (0); confluent with the pedicle of the malleus (1).

119. Ventral margin of sigmoid process in lateral view: present as a distinct margin (0); absent with the lateral margin of the sigmoid process turning smoothly into a sulcus on the lateral side of the bulla (1).

120. Shape of conical process in lateral view: well developed and dorsally convex (0); reduced to a low ridge or absent (1).

121. Elliptical foramen: present (0); absent (1).

122. Relative position of lateral and medial lobes or lateral lobe and involucral ridge: equally project posteriorly (0); lateral lobe projects farther posteriorly (1).

123. Medial lobe of tympanic bulla: present as distinct lobe or prominence on the involucrum (0); absent or indistinct (1).

124. Crest connecting medial and lateral lobes of tympanic bulla in posterior view: present (0); absent (1).

125. Orientation of crest connecting medial and lateral lobes of tympanic bulla in posterior view: roughly parallel to the plane connecting the ventral surfaces of the medial and lateral lobes (0); oriented at an angle to the plane connecting the ventral surfaces of the medial and lateral lobes (1).

126. Lateral lobe of bulla in posterior view: distinctly narrower than medial lobe (0); medial and lateral lobes are subequal in size or medial lobe is smaller (1).

127. Anteriormost point of involucral ridge: extends anteriorly to form the anteriormost point of the bulla (0); in line with or posterior to the anterior border of the bulla (1).

128. Dorsolateral surface of involucrum: divided into a low anterior and an elevated posterior part separated by a clearly defined step (0); forms a continuous rim (1).

129. Transverse creases on dorsal surface of involucrum: poorly developed or absent (0); well defined and deep (1).

130. Development of tympanic sulcus: developed as a faint line (0); forms a distinct crest or sulcus (1).

131. Outline and position of tympanic sulcus: forms a semicircular and ventrally curved line well separated from the intersection of the conical and sigmoid processes (0); forms a roughly horizontal line at or close to the level of the intersection of the conical and sigmoid processes (1).

132. Anteroventral side of tympanic bulla: transversely convex (0); distinctly flattened or slightly concave (1).

133. Transversely concave depression anteromedial to Eustachian outlet: present (0); absent with the surface medial to the Eustachian outlet being flat or convex (1); absent with the medial border of the Eustachian outlet reduced to a thin wall (2).

134. Anterolateral ridge or shelf: absent (0); present (1).

Mandible

135. Medial surface of central part of mandible: similar to lateral surface (0); distinctly flattened relative to lateral surface (1).

136. Mandibular symphysis: sutured or fused (0); not sutured (1).

137. Outline of posterior part of mandible in dorsal or ventral view: follows a straight line or simple curve (0); sigmoidal owing to a laterally reflexed neck and condyle (1).

138. Horizontal ramus of mandible in dorsal or view: bowed medially (0); straight (1); bowed laterally (2).

139. Anterior extremity of mandible: vertical or slightly twisted with the ventral edge shifted medially (0); apex of mandible shifted to an almost horizontal position (1).

140. Horizontal ramus of mandible in lateral view: height of ramus remains roughly constant throughout (0); arched dorsally (1); increases in height anteroposteriorly (2); dorsoventrally constricted near the center (3).

141. Mandibular foramen: dorsoventral height approximately that of the horizontal ramus thus forming a mandibular fossa (0); dorsoventral height about half that of the horizontal ramus or less (1).

142. Anterior border of mandibular foramen: round (0); triangular (1); sigmoidal with the dorsal border of the foramen developed into a roof (2).

143. Relative position of anterior border of mandibular foramen: in line with coronoid process (0); posterior to coronoid process (1).

144. Subcondylar furrow: absent (0); present medially only (1); deep groove on the posterior surface separating the condyle and angular process medially and laterally (2).

145. Coronoid process in lateral or medial view: forms a broad plate with a convex anterior border (0); sharply triangular and about as high as long (1); bluntly triangular and much longer than high (2); shaped like a finger and pointing posteriorly (3).

146. Postcoronoid elevation: absent (0); present (1).

147. Position of angular process: located below the condyle or slightly anterior (0); projects posteriorly to a level posterior to the condyle (1).

148. Orientation of articular surface of mandibular condyle: posterior (0); posterodorsal (1); dorsal with the condyle being confluent with a dorsoventrally expanded angular process (2); dorsal with the condyle being larger than and clearly offset from the angular process (3).

149. Sulcus for attachment of mylohyoid muscle on ventromedial surface of mandible: absent (0); present (1).

Postcranial skeleton

150. Height of transverse process of atlas at base: more than half the height of the articular surface (0); equal to half the height of the articular surface or less (1).

151. Foramen transversarium in axis: absent (0); present (1).

152. Cervical vertebrae: separate or partially separate (0); fused (1).

153. Lower transverse process on seventh cervical vertebra: present (0); absent (1).

154. Orientation of transverse processes of lumbar vertebrae: oriented ventrolaterally (0); oriented laterally and horizontally (1).

155. Shape of transverse processes of lumbar vertebrae: slender and distinctly wider transversely than long anteroposteriorly (0); shaped like a broad plate and roughly as wide transversely as long anteroposteriorly (1); wider than long with a distinct projection on their anterior borders (2).

156. Sternum: composed of several bones (0); composed of one bone (1).

157. Proportions of scapula: anteroposterior length approximately equals or is less than its maximum dorsoventral height (0); maximum anteroposterior length clearly exceeds its maximum dorsoventral height (1).

158. Coracoid process of scapula: present (0); absent (1).

159. Acromion process of scapula: present (0); absent (1).

160. Supraspinous fossa of scapula: present (0); absent or nearly absent with acromion process located near anterior edge of scapula (1).

161. Deltoid crest of humerus: present as a distinct crest (0); absent or reduced to a variably developed rugosity (1).

162. Humerus: longer than or roughly same length as radius and ulna (0); shorter than radius and ulna (1).

163. Orientation of humeral head in lateral or medial view: angled (0); vertical (1).

164. Distal portion of humerus in lateral view: distal epiphysis narrower than shaft (0); distal epiphysis flared compared to shaft (1).

165. Olecranon process: present as a distinct process (0); absent (1).

166. Manus: pentadactyl (0); tetradactyl (1).